Seasonal and Interannual Subsurface Temperature Variability off Peru, 1952 to 1984

R.E. BRAINARD*
D.R. McLAIN**
Pacific Fisheries Environmental Group
Southwest Fisheries Center
National Marine Fisheries Service, NOAA
P.O. Box 831
Monterey, California 93940, USA

Abstract

Time series of monthly means of subsurface ocean temperature data along the Peru coast are developed for the period 1952 to 1984 for historical studies of anchoveta populations. Monthly mean values of sea surface temperature (SST), depth of the 14oC isotherm, and thickness and heat content of the surface layer were computed from all available subsurface temperature profiles. Means of these four parameters were computed for five areas along the Peru coast from 1 to 17oS, extending approximately 300 km offshore. Intra-annual (seasonal) and interannual variations of the four parameters are described and plotted as contour isograms. Time series of the four parameters are presented for the region from 4 to 14oS, as are monthly means of the Southern Oscillation Index and SST and sea level at Talara and La Punta (Callao), Peru.

Introduction

The coastal waters off the west coast of South America, particularly off Peru, are among the most biologically productive regions of the world's oceans (Ryther et al. 1971). The Peruvian anchoveta *(Engraulis ringens)* once supported the world's largest fishery. The high productivity of the area is a result of coastal upwelling which is an oceanic response to the southeasterly trade winds which cause offshore Ekman divergence, elevating the thermocline and bringing relatively cold, nutrient-rich water to the euphotic zone where the nutrients can be utilized by phytoplankton photosynthesis (Barber et al. 1985). The upwelling ecosystem off Peru is subject to considerable natural variability, with prominent time scales ranging from days to decades. This paper examines two temporal scales of oceanic variability which are likely to affect populations of anchoveta: seasonal (months) and interannual (years). The seasonal or intra-annual variability, being strongly dependent upon the annual solar cycle, is relatively predictable, and therefore likely to promote evolutionary adaptation (Parrish et al. 1983; Bakun, this vol.). The interannual variability, by contrast, has an irregular period which would tend to promote population variations. The dominant form of interannual variability off Peru occurs when the normal seasonal upwelling of nutrients is interrupted by "El Niño" intrusions of relatively warm, clear oceanic waters from the west and north.

The coastal upwelling off Peru is imbedded within the Peru current system, which consists of several more or less independent currents interacting in a rather complicated manner (Wyrtki 1966). Gunther (1936) first distinguished a poleward countercurrent situated between the northwestward flowing Peru Coastal Current and the northwestward flowing Peru Oceanic Current farther offshore. This intermediate current, the Peru Countercurrent or Gunther Current, is a weak and irregular southward flow along 80°W and is usually observed only as a subsurface current. At the surface it is usually concealed by the wind drift to the northwest and west. It is strongest near 100 m depth, but reaches to about 500 m.

According to Wyrtki (1965, 1966), the Peru Coastal Current flows northwestward along the coast with velocities of 10-15 cm/s. At about 15°S, much of this flow turns westward away from the coast and increases speed to 25-35 cm/s as it joins the South Equatorial Current. Generally, the Peru Coastal Current is strongest from April to September. North of 15°S, the wind drift remains northwestward, but it is shallow and the southward flow of the Peru Undercurrent lies immediately beneath the shallow surface layer. The combined system of the Peru Coastal Current, the westwardwind drift, and the subsurface Peru Countercurrent maintain the upwelling along the coast. North of 15°S, the upwelling is supplied by equatorial subsurface water which is of high salinity and low oxygen content and flows southward in the Peru Countercurrent. The Peru Oceanic Current, which flows in a more westward direction and is slightly stronger than the Peru Coastal Current, seems to have little direct interaction with the more complicated processes closer to the coast.

The mean topography of the thermal structure of the Eastern Tropical Pacific reflects the ocean currents and has been described by Wyrtki (1966). The thermocline is relatively shallow along the coast at depths of 40 to 60 m and slopes downward in the offshore direction to depths of over 200 m about 1,000 km offshore. A region of shallow thermocline extends westward from the coast along the equator out to 130°W and beyond.

The current system off Peru is related to the large-scale oceanic and atmospheric circulations over the entire tropical Pacific. The atmospheric circulation over the region is dominated by the Hadley circulation of rising air over the equatorial region and sinking air over mid-latitudes near 30°N and 30°S. The Hadley circulation creates the high-pressure systems observed over the oceans in these latitudes which are strongest in the summer and weakest in the winter of their respective hemispheres. The meridional Hadley circulation is modified by zonal Walker circulation of rising air over the warm western tropical Pacific (WTP) and sinking air over the cold, upwelled water of the eastern tropical Pacific (ETP). The zonal Walker circulation normally causes heavy rainfall and low pressure over the WTP and sparse rainfall and high pressure over the ETP. The trade winds result from the combination of the Hadley and Walker circulations: the trades blow equatorward from the mid-latitude oceanic highs toward the lower pressure at the equator and westward from the higher pressure over the ETP to the lower presure over the WTP.

The surface wind stress created by the northeast and southeast trade winds drive the warm surface water westward in the North and South Equatorial Currents, respectively. This westward transport of mass and heat depresses the thermal structure and raises the sea level in the WTP. By conservation of mass, the high sea level in the WTP requires a poleward flow of the western boundary currents of the North and South Pacific gyres and eastward flow in the North and South Equatorial Countercurrents and the equatorial Undercurrent or Cromwell Current (within a degree or so of the equator).

The zonal slope of the sea surface downward from the high sea levels in the WTP to the lower sea levels in the ETP establishes a reverse zonal slope of the thermocline upward from the WTP to the shallow thermocline of the ETP. Meyers (1979) showed that near the equator (between 1°N and 1°S), the 14°C isotherm varies from depths of 200 to 250 m in the WTP to depths of 100 to 150 m in the ETP. Off the South American coast, local alongshore winds induce offshore Ekman divergence and the associated upwelling. This upwelling elevates the relatively shallow thermocline, bringing nutrient-rich deep water to the euphotic zone where it supports a high level of biological productivity. In addition, the trade winds cause oceanic divergence or surface transport away from the equator. This divergence forces local upwelling along the equator, which produces a region of shallow thermocline and above normal productivity that extends westward along the equator from the coast.

Interannual variations of the stength of the trade winds cause changes in the ocean circulation and related changes in the upwelling of nutrients off Peru. According to the hypothesis of Wyrtki (1975), El Niño occurs when a weakening or reversal of the trades occurs after a sustained period of anomalously strong trades. The period of stronger than normal winds forces an even greater than normal east to west slope of the sea surface. When the trade winds slacken or reverse, the forcing of the higher than normal sea levels in the WTP is removed. This imbalance generates equatorially-trapped baroclinic disturbances which propagate eastward along the equator in the form of equatorial Kelvin waves (Enfield and Allen 1980). The propagation of these long-period internal waves, and the associated energy, across the entire equatorial Pacific from Indonesia to South America has been observed using an extensive array of sea level monitoring stations (Wyrtki and Nakahara 1984). Upon encountering the South American coast, this energy is observed as a large intrusion of warm water which depresses the normally shallow thermocline and causes a rapid rise in sea level along the coast. As a result, normally arid regions of Peru and Ecuador receive inordinate amounts of rain, with severe flooding occurring during major events.

Interannual variations in the strength of the trade winds are part of a global pattern of surface pressure variation called the Southern Oscillation. The Southern Oscillation is often measured by the difference of atmospheric pressure between weather stations in the ETP and WTP. Quinn (1974) and Quinn and Neal (1983) have used the difference of atmospheric pressure between Easter Island (representative of the Indonesian low) as an index of the Southern Oscillation (SOI, see Table 1). Quinn (1974) demonstrated the strong relationship between anomalously low SOI values and the occurrence of El Niño off the coasts of Peru and Ecuador. A time series of anomaly of the SOI pressure difference shows the major El Niño events of recent decades (Figs. 1 and 2). Note the strong positive SOI presure differences (and implied strong trade winds) during 1954-1956 and 1970-1971. Subsequent sharp declines in the SOI pressure difference in the winters of 1956-1957 and 1971-1972 were followed by El Niño events, as evidenced by the increased SST and sea level a. Talara and La Punta. Also, note that the strong 1982-1983 El Niño was not preceded by a period of strong positive SOI, rather, it occurred during a period of predominantly negative SOI which began in 1976.

The formation of El Niño has been modelled numerically by McCreary (1976) who suggested that the anomalous deepening of the density structure observed during El Niño events dissipates by reflection in the form of westward propagating baroclinic Rossby waves and transmission to the north and south along the coast as low-frequency coastally trapped waves and coastal Kelvin waves. Such baroclinic waves can be observed as anomalous deepenings of temperature and salinity surfaces adjacent to the coast and as anomalous rises of sea level at coastal tide stations. Poleward currents along the coast are created in geostrophic response to the anomalous deepening and change in slope of the density surfaces normal to the coast. The currents reverse to equatorward as the anomalous deepening dissipates. To some extent these processes occur each year and anomalous warm years are merely an extreme condition of the normal annual cycle of events (Chavez et al. 1984).

Although the interannual changes associated with El Niño events are dominant, longer period fluctuations also occur. In their 34-year time series of temperature at 100 m along the west coast from British Columbia to Chile, Brainard and McLain (1985) showed a marked warming trend occurring between the early and late 1950s, cooling in the 1960s, and warming again in the mid-1970s and early 1980s (see also Tables 2 and 3). The causes of these long-term temperature trends are unknown, but like the interannual variations, they are related to changes in both the large-scale atmospheric and oceanic circulations. The period of below normal SOI pressure differences during the years 1976-1983 (Fig. 2) is an example. El Niño-like conditions of above normal SST and sea level occurred during much of this period in the northeast Pacific (McLain 1983, and see Fig. 2 and Tables 4 and 5 for monthly sea level data from 1950 to 1974).

Development of historical time series of subsurface temperature conditions off Peru is important for modelling historical changes in fish populations of the area. This paper presents plots and tables of monthly mean values of four parameters computed from subsurface temperature observations for 1952 to 1984 for use in historical studies. These four parameters are SST, depth of the 14°C isotherm, depth to the temperature that is 2.0°C less than the surface temperature (SST-2°C), and heat content from the surface to the SST-2°C isotherm. The depth

Table 1. Southern Oscillation Index (SOI). Monthly mean pressure difference in millibars between Easter Island and Darwin, Australia. Data courtesy of Dr. W. Quinn, Oregon State University.

Year	Jan	Feb	Mar	Apr	May	Jun	Jul	Aug	Sep	Oct	Nov	Dec
1948	12.9	11.7	12.3	10.4	9.3	11.6	10.7	11.2	9.3	12.1	9.8	9.3
1949	8.0	12.8	15.0	6.2	7.8	11.9	10.3	9.7	11.7	11.3	13.4	15.1
1950	16.4	17.6	15.0	14.7	9.5	13.8	11.3	9.2	9.1	16.0	17.1	17.6
1951	14.3	14.3	12.9	7.3	4.1	7.8	4.6	5.2	5.4	9.9	13.6	11.8
1952	13.2	11.5	10.8	5.5	8.6	7.0	10.9	8.9	5.8	11.6	12.8	11.3
1953	12.6	9.1	12.1	8.3	6.1	8.4	6.7	5.0	8.2	16.2	12.8	12.8
1954	15.4	15.2	10.6	11.0	10.7	7.1	11.0	8.6	13.8	15.3	14.9	16.3
1955	11.2	18.6	13.9	13.2	10.9	10.6	10.0	11.7	16.2	16.8	13.3	15.1
1956	15.9	15.3	13.6	12.3	12.7	8.0	9.1	10.5	10.7	11.8	10.5	9.8
1957	10.2	10.8	10.0	7.7	3.9	4.1	7.0	8.6	8.6	11.8	9.4	11.5
1958	11.0	13.4	11.3	6.1	3.4	10.3	2.9	10.8	8.6	12.0	13.4	8.5
1959	15.0	11.1	10.1	11.7	5.5	10.0	5.9	11.3	8.5	11.2	13.8	14.5
1960	11.0	12.5	9.4	9.1	8.3	5.4	9.3	9.7	12.5	12.7	12.6	10.5
1961	12.3	14.9	9.5	13.0	4.8	4.4	1.6	4.0	10.0	10.1	11.5	12.0
1962	12.4	11.1	10.6	10.2	10.6	7.5	7.3	11.0	13.0	14.2	10.6	13.2
1963	16.2	13.5	14.9	8.2	5.0	6.0	11.9	7.9	7.5	7.7	12.9	10.6
1964	12.3	13.0	13.0	11.1	6.4	9.9	8.7	11.2	13.1	10.3	9.5	12.8
1965	12.5	12.9	10.1	8.0	4.5	3.2	3.2	6.3	6.7	11.3	8.3	10.2
1966	10.5	13.7	10.4	7.8	3.3	10.4	5.0	10.3	12.0	10.4	11.1	13.8
1967	14.3	15.5	12.7	6.3	9.1	11.6	13.9	11.0	12.5	10.7	11.0	12.5
1968	15.9	12.9	14.8	8.3	7.5	10.8	8.3	6.3	4.8	12.0	10.2	12.7
1969	10.2	14.7	12.7	7.1	6.0	6.3	3.5	8.6	8.2	10.5	15.9	13.1
1970	12.8	12.8	9.8	7.0	12.4	10.2	10.2	10.0	11.9	13.3	16.5	16.8
1971	15.5	16.0	15.2	11.2	14.3	11.1	5.2	12.0	12.7	11.3	14.5	15.1
1972	10.4	11.5	13.4	7.5	.6	.3	5.5	3.2	4.8	8.2	10.2	8.9
1973	12.5	12.7	13.0	8.9	7.6	9.5	8.4	10.7	13.6	13.0	16.2	16.5
1974	16.8	17.1	15.4	9.5	6.1	10.1	9.4	5.3	11.2	13.4	15.7	13.0
1975	11.6	8.6	13.8	8.7	3.8	8.6	8.8	13.4	13.3	14.0	13.6	14.9
1976	14.5	15.0	13.7	6.7	2.4	3.5	3.1	8.2	5.2	7.2	11.0	7.6
1977	10.2	15.0	8.0	5.3	2.3	5.9	11.1	10.0	4.8	7.0	11.5	10.5
1978	13.1	9.7	9.6	6.0	7.8	9.1	7.6	10.7	10.3	6.9	9.1	11.6
1979	11.0	13.1	10.9	4.5	3.7	9.7	2.7	1.1	9.2	10.1	8.3	9.9
1980	13.6	12.2	9.4	8.6	7.4	7.5	6.6	7.3	6.5	12.4	10.3	10.5
1981	16.5	15.0	8.0	7.3	7.6	6.4	8.0	7.4	6.2	9.5	13.6	13.2
1982	14.2	14.4	12.2	4.2	6.3	6.9	2.9	1.5	4.0	6.8	5.3	7.2
1983	3.9	4.3	7.3	7.2	5.8	6.4	4.6	9.0	10.9	10.5	12.4	10.5
1984	9.9	13.6	10.9	5.6	7.0	6.6	8.4	6.5	6.5	10.6	12.5	14.2
1985	13.1	14.2	13.4	12.7	8.3	4.8	5.9	13.0	10.1	****	****	****

of the SST-2°C isotherm indicates the thickness of the mixed layer which provides a measure of the depth of the thermocline and hence, relates to upwelling and availability of nutrients to the euphotic zone. This definition of mixed layer is similar to that used by Robinson and Bauer (1976), except that they chose the depth that is 2°F (1.1°C) less than the SST. The SST-2°C depth was selected for defining the depth of the thermocline from smooth average temperatures because 2°C is larger than the small positive and negative temperature changes near the surface that are present in both the raw data and the analyzed values. Also, a temperature change of 2°C is large enough to reach the large gradients found in the thermocline.

The 14°C isotherm is at depths of 80 to 180 m off Peru and is below the strongest gradients of the thermocline. Variations in the depth of the 14°C isotherm are indicators of large-scale vertical movements of the water column, such as upwelling. Also, Barilotti et al. (1984) related the depth of the 14°C isotherm off San Diego, California, to the depth of the thermocline and hence to the supply of nutrients for kelp growth.

Heat content down to SST-2°C is an indicator of the overall environmental change in the euphotic zone. Combined with wind-derived Ekman transports (Bakun, this vol.; Mendo, this vol.), these vertical temperature parameters can be used to describe the offshore velocity structure which is critical to the reproductive success of the anchoveta (Parrish et al. 1983, and other contributions in this vol.).
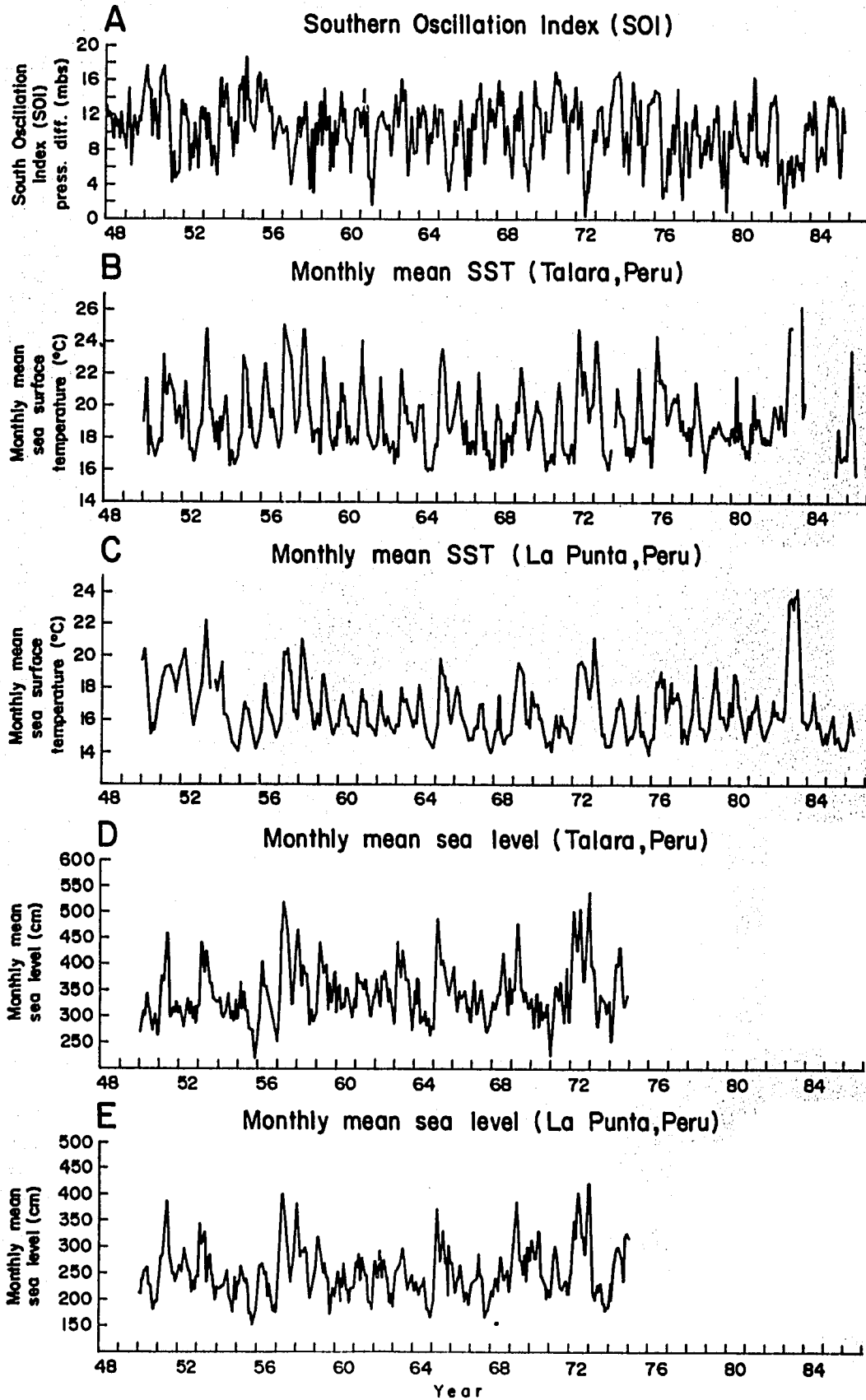
Fig. 1. Time series of monthly means of (A) Southern Oscillation Index (difference of surface barometric pressure in millibars between Easter Island and Darwin, Australia), (B and C) SST in degrees C, and (D and E) sea level in cm at Talara and La Punta, Peru. Values are computed as monthly means of daily observations.
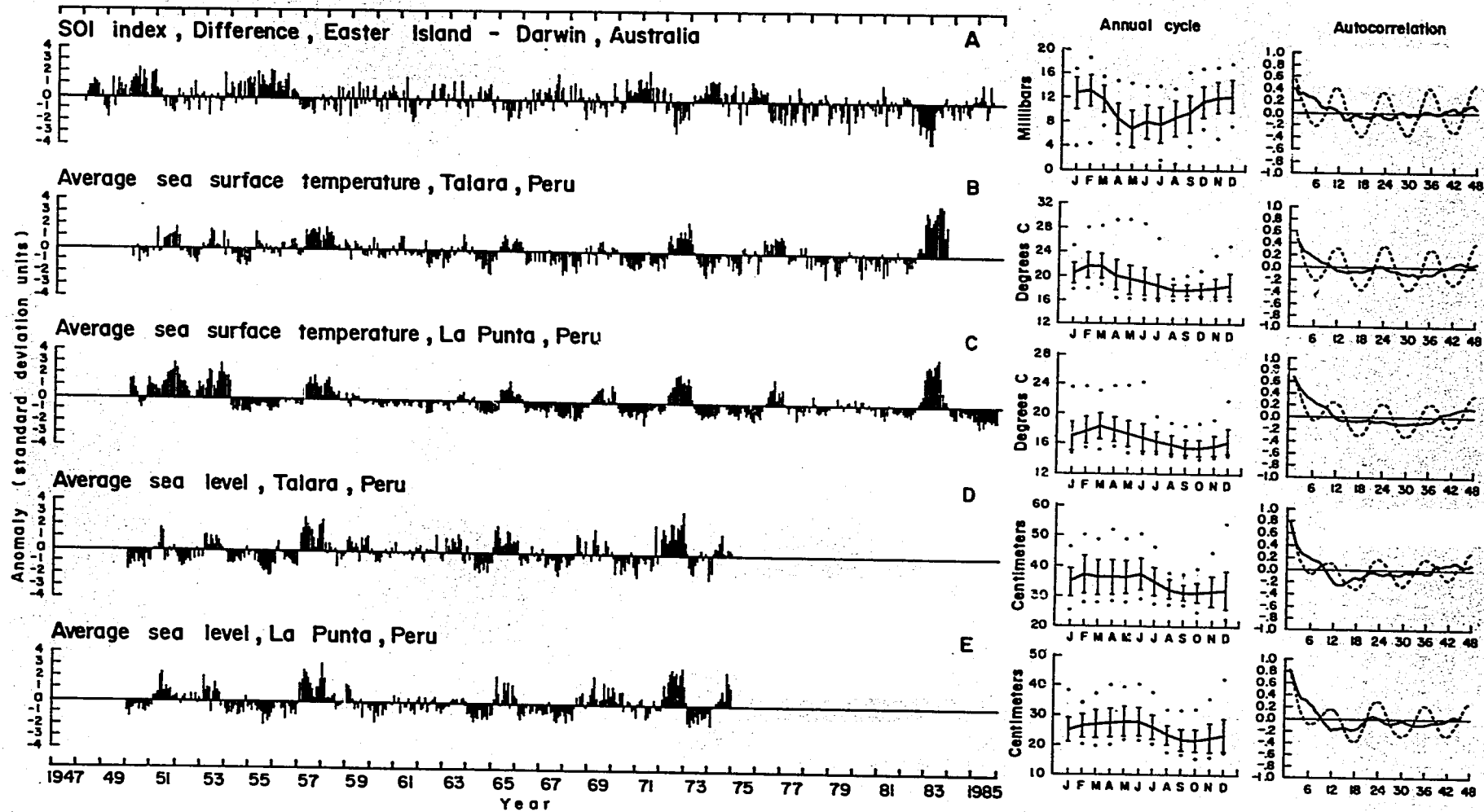
Fig. 2. Annual cycles, autocorrelation functions, and anomalies of monthly means of daily observations at coastal and island stations. Parameters are (A) Southern Oscillation Index, (B and C) SST, and (D and E) sea level at Talara and La Punta, Peru. The annual cycle plot (center) shows the long term (1943-1986) monthly means, between-year standard deviations (bars), and range of interannual variability (dots). The autocorrelation function plot (right) shows the autocorrelation of each original data series (dotted) and the autocorrelation of each anomaly series (solid). The time series of anomalies from 1941-1986 mean (left) are shown in standard deviation units for intercomparison between data series. Based on data in Tables 1-5.

19

Mean values of the four parameters were computed for each month for the 33-year period from 1952 to 1984 for five areas along the coast from 1 to 17ºS (Fig. 3). Each of the given areas spanned 3 degrees of latitude except for the central-most area which spanned 4 degrees. The zonal extent of each area was chosen so that they would extend about the same distance offshore, roughly 300 km. In addition, all data prior to 1952 were combined to form a single composite year. Thus, the resulting fields of monthly means for each parameter for the 5 areas covers 34 years (408 months), for a total of 2,040 cells. The average value for the region from 4 to 14ºS was obtained by averaging the values computed for the three central areas. Mean temperature at 25 m depth intervals from the surface to 350 m were also computed for the central area to show vertical variations of temperature with time. The data are plotted as contour isograms of latitude (area) or depth vs. month to show both seasonal and interannual variations.

Table 2. Monthly mean sea surface temperature in degrees Celsius at Talara, Peru. Data courtesy of Dr. D. Enfield, Oregon State University.
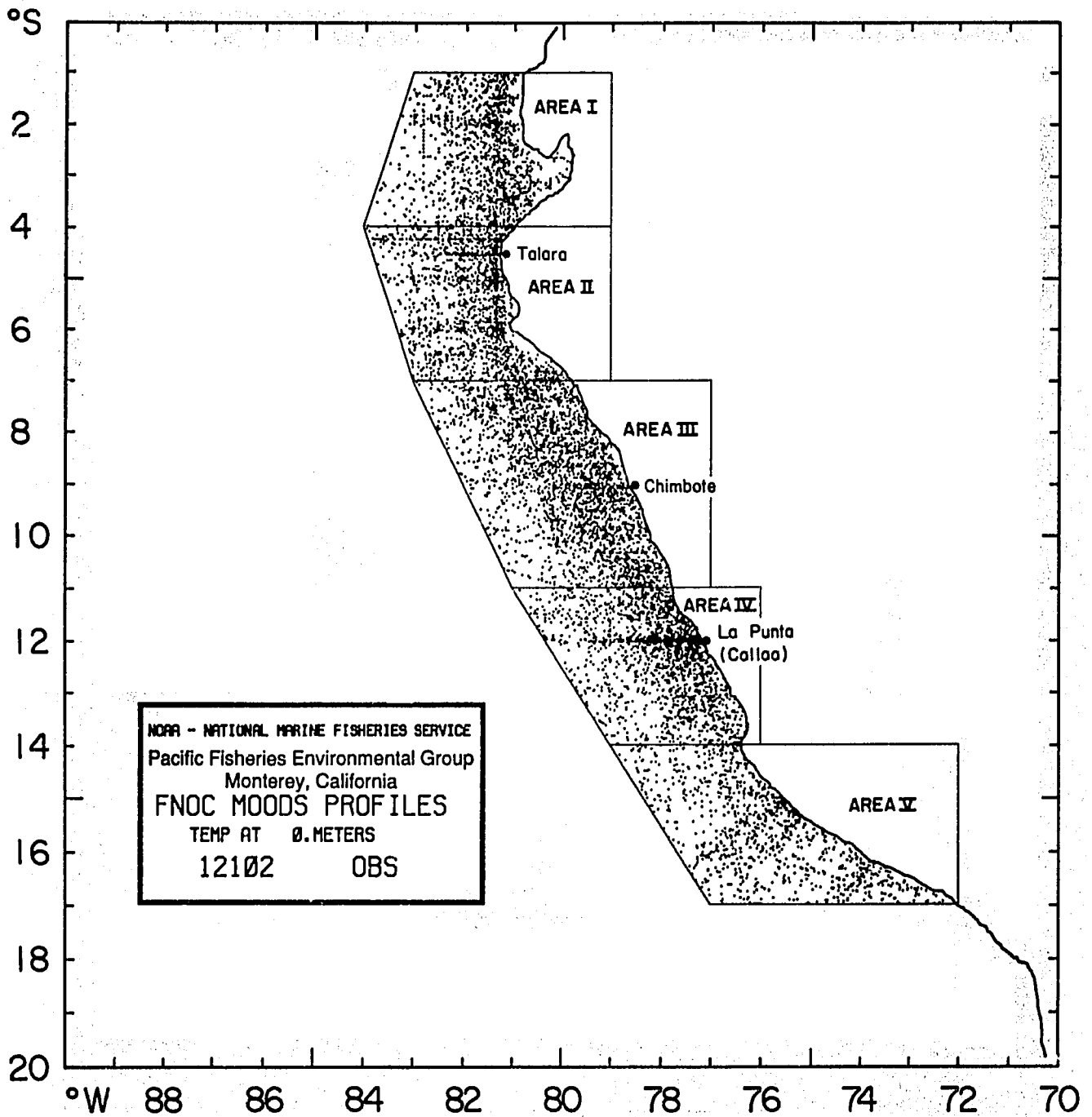
Year	Jan	Feb	Mar	Apr	May	Jun	Jul	Aug	Sep	Oct	Nov	Dec
1950	19.0	21.6	21.7	16.9	18.6	17.6	17.3	16.8	17.6	17.9	17.7	18.1
1951	23.2	20.6	20.9	21.9	21.4	21.1	20.5	18.8	18.9	19.8	19.6	17.9
1952	19.8	21.4	20.6	18.4	17.2	17.3	16.5	16.5	17.1	17.7	18.6	18.8
1953	20.8	23.0	24.8	23.6	19.7	19.7	18.8	17.7	19.0	17.2	19.2	18.4
1954	19.5	20.6	20.4	17.2	16.2	17.1	16.4	16.3	16.7	16.7	17.9	18.2
1955	22.8	22.9	22.4	20.9	18.6	19.7	18.0	17.8	17.3	17.4	18.3	17.9
1956	19.2	22.6	22.5	20.3	19.5	19.3	19.8	18.5	18.1	17.4	17.4	17.9
1957	20.7	25.1	24.3	23.9	23.4	22.8	21.0	19.4	18.3	19.1	19.4	22.1
1958	22.8	24.8	23.8	21.0	19.9	19.7	18.2	17.7	18.4	18.4	18.6	17.0
1959	20.3	23.0	22.4	20.6	19.9	18.1	17.5	17.2	18.0	17.5	19.6	18.6
1960	21.3	20.3	20.6	18.7	17.7	18.7	17.6	17.7	18.0	17.8	17.6	19.6
1961	22.4	24.1	20.7	20.1	18.9	18.1	17.8	17.6	17.3	17.5	17.5	18.1
1962	21.8	19.3	18.7	17.6	18.2	17.5	17.1	17.3	17.8	16.4	17.2	16.8
1963	19.4	22.3	20.8	19.6	19.9	18.9	19.0	19.0	18.4	17.8	17.9	19.2
1964	20.1	19.9	20.1	18.5	16.1	16.0	16.1	16.0	16.0	17.0	17.6	17.5
1965	20.3	22.5	23.3	23.5	22.0	19.8	18.6	18.3	18.5	19.1	19.4	20.2
1966	21.2	21.5	19.4	17.9	17.6	19.1	17.0	17.7	17.0	17.8	17.2	17.1
1967	20.5	22.1	19.4	18.5	17.3	18.4	16.9	17.1	16.1	16.4	16.1	18.1
1968	20.1	19.3	19.1	16.2	17.9	16.6	18.3	17.8	18.1	17.0	19.0	18.4
1969	20.2	19.7	22.4	22.3	21.6	19.7	18.2	17.3	17.5	18.4	18.8	19.2
1970	20.3	19.8	19.6	19.3	18.0	16.8	16.0	16.5	16.5	17.0	16.5	16.5
1971	19.5	20.5	21.5	20.5	17.5	17.0	17.0	17.0	16.5	17.5	17.5	16.5
1972	19.8	23.9	24.8	22.3	20.7	22.2	21.0	19.5	19.0	19.9	20.1	23.3
1973	24.0	23.6	21.9	19.4	17.9	16.9	16.7	16.2	16.0	17.0	17.3	16.0
1974	18.8	21.2	20.4	19.5	19.4	19.1	18.0	16.9	17.4	16.6	17.4	16.9
1975	17.8	18.6	22.4	21.5	19.8	17.8	18.0	17.7	18.1	18.1	16.2	17.7
1976	20.5	24.4	23.6	21.4	21.7	21.2	21.2	19.0	18.9	19.5	20.1	20.3
1977	20.5	20.3	20.8	19.4	18.5	19.1	18.2	18.3	17.9	18.7	16.9	18.7
1978	18.7	21.5	20.1	19.1	18.6	17.3	17.2	15.9	17.3	17.8	18.2	18.1
1979	18.7	18.3	18.7	19.0	18.7	18.3	18.2	18.1	17.9	18.0	17.6	18.5
1980	18.6	17.8	21.8	17.8	19.0	18.4	17.4	17.5	16.8	17.2	16.7	18.9
1981	17.7	20.7	18.6	19.2	19.1	18.7	17.7	18.0	17.6	17.9	17.7	17.7
1982	18.4	19.9	19.9	19.6	18.7	20.0	20.0	18.5	18.2	20.9	23.4	24.9
1983	24.9	27.9	28.3	29.2	29.2	28.5	26.2	19.3	20.1	****	****	****
1984	****	****	****	****	****	****	****	****	****	****	****	****
1985	****	****	****	****	15.7	18.6	17.0	16.6	16.7	16.9	16.7	18.6
1986	20.2	23.5	19.4	18.8	15.7	****	****	****	****	****	****	****

Fig. 3. Locations of five areas along the Peru coast for which subsurface temperature profiles were extracted from the FNOC MOODS and used to perform analyses of surface and subsurface temperature. A total of 12,102 profiles were extracted from the MOODS files for all five areas for SST analyses. Area I is the northernmost area and Area V, the southernmost.

Table 3. Monthly mean sea surface temperature in degrees Celsius at La Punta, Peru. Data courtesy of Dr. D. Enfield, Oregon State University.

Year	Jan	Feb	Mar	Apr	May	Jun	Jul	Aug	Sep	Oct	Nov	Dec
1950	19.8	20.4	19.6	18.3	16.3	15.1	15.6	15.4	16.3	17.2	17.2	17.9
1951	18.7	18.9	19.3	19.3	19.4	19.2	18.9	18.5	17.7	18.7	19.2	19.2
1952	19.5	20.0	20.4	19.2	18.1	16.7	16.0	15.7	15.9	16.8	16.9	17.9
1953	18.2	20.3	22.3	21.5	19.0	18.0	****	****	18.4	17.8	18.3	19.2
1954	19.6	16.3	16.4	16.2	15.5	15.2	14.7	14.5	14.4	14.2	14.1	15.2
1955	15.9	16.5	17.1	16.7	16.6	15.9	15.6	15.0	14.4	14.2	14.7	15.1
1956	15.4	17.2	18.2	17.8	16.7	16.5	16.0	15.8	15.3	14.9	15.2	15.5
1957	15.9	19.2	20.2	20.0	20.4	19.1	18.9	17.5	16.5	16.6	16.1	18.3
1958	19.9	21.0	20.0	18.9	18.1	17.3	17.1	15.9	15.5	15.4	16.4	15.7
1959	15.8	18.4	18.8	18.1	17.7	16.5	16.0	15.5	15.2	15.2	15.7	15.6
1960	16.7	17.2	17.6	16.9	16.2	16.1	15.6	15.6	15.4	15.1	15.2	15.0
1961	16.2	17.6	17.9	17.1	17.2	15.9	15.6	15.7	15.5	15.4	15.1	15.3
1962	16.8	17.8	16.5	16.1	15.7	16.3	16.0	15.6	15.5	15.4	15.1	15.3
1963	15.6	16.3	18.1	17.3	17.1	17.3	16.9	16.5	15.5	15.4	15.2	15.7
1964	17.3	18.2	17.3	16.7	15.8	15.4	14.9	14.7	14.6	15.6	15.9	15.8
1965	15.4	16.5	19.9	19.6	18.9	18.6	17.8	18.0	16.4	14.3	14.5	14.9
1966	17.9	18.1	17.6	16.5	16.1	15.9	15.6	15.1	14.8	15.9	16.6	17.4
1967	15.6	15.5	17.0	17.0	17.0	15.5	15.3	14.6	14.3	14.9	14.8	15.4
1968	15.3	15.4	17.6	15.5	14.9	14.6	14.6	15.0	15.1	14.0	14.1	14.6
1969	17.4	18.6	19.5	19.6	19.2	19.1	16.7	15.8	15.9	15.1	15.4	16.4
1970	16.9	17.0	17.0	16.1	16.1	15.6	15.0	14.5	14.4	15.6	17.8	17.8
1971	15.5	16.3	15.1	16.0	16.3	15.8	15.6	15.5	15.3	14.7	14.1	14.8
1972	16.0	17.6	19.5	19.5	19.7	19.4	19.3	18.8	17.9	14.8	14.8	15.3
1973	21.1	20.5	19.0	17.4	16.2	15.1	15.2	14.4	14.4	17.4	18.2	19.0
1974	15.3	15.8	16.8	16.8	17.3	16.9	16.3	15.5	14.7	14.4	14.4	14.8
1975	15.3	15.6	17.2	17.6	16.6	15.1	15.3	14.7	14.2	14.6	15.0	14.9
1976	14.8	16.9	18.4	18.2	18.5	19.0	18.1	18.6	15.9	13.9	14.8	14.9
1977	17.1	17.4	17.3	17.7	17.2	16.6	14.6	15.5	15.0	16.6	16.9	18.3
1978	16.2	17.7	19.5	18.1	16.5	15.6	15.5	15.5	14.8	14.6	15.3	15.6
1979	17.0	17.8	19.4	17.9	17.6	16.2	16.2	16.2	15.8	15.1	15.5	16.2
1980	16.3	16.9	18.9	18.6	17.3	16.7	16.4	15.6	15.3	15.5	15.7	17.2
1981	15.5	16.6	16.5	16.8	17.6	16.7	15.7	15.4	14.9	14.7	15.7	16.3
1982	15.6	16.3	17.3	16.4	16.6	16.2	16.2	16.2	16.0	14.9	15.3	15.5
1983	23.5	23.6	23.0	23.7	23.8	24.2	19.6	17.4	16.0	16.5	19.0	21.7
1984	15.8	16.1	16.7	17.9	16.4	15.6	15.8	15.5	14.8	16.0	15.9	15.5
1985	15.1	15.5	15.5	16.3	14.7	14.7	15.0	14.7	14.3	14.6	15.2	14.7
1986	14.7	16.6	15.9	15.3	15.2	****	****	****	****	14.3	14.2	14.3

Data Acquisition and Processing

Data Sources

The profiles of subsurface temperature for the Peru coastal region were acquired from the US Navy Fleet Numerical Oceanography Center (FNOC) in Monterey, California. The profiles were obtained by merchant, naval and research vessels of many nations using a variety of sampling instruments, including bottle casts, mechanical bathythermographs (MBT), expendable bathythermographs (XBT) and electronic conductivity/temperature/depth profiles (CTD). The capability and accuracy of these instruments vary widely: MBTs, with typical accuracies of 0.3 to 1.0°C, were used until the development of XBTs in the 1960s. Generally, MBTs reached depths of only 100-200 m, whereas the newer XBTs are capable of depths to 450, 700, or even 1,500 m. The accuracy of XBTs are typically 0.1 to 0.4°C. Bottle casts and CTD casts from research vessels are capable of any depth, with typical cast depths to 1,000 or 1,500 m and accuracies of 0.001 to 0.1°C. Profiles from all of these sources are normally mailed to oceanographic data centers and assembled into common data sets. The time lag between observation and final assembly of the data by the data centers may be 5 to 10 years or longer. To reduce this time lag, many of the profiles are manually digitized and transmitted by radio in near

Table 4. Monthly mean sea level (cm) at Talara, Peru. Data courtesy of Dr. D. Enfield, Oregon State University.

Year	Jan	Feb	Mar	Apr	May	Jun	Jul	Aug	Sep	Oct	Nov	Dec
1950	267	287	310	301	342	318	310	294	275	303	272	264
1951	344	373	366	386	460	4:0	303	301	317	307	328	307
1952	315	302	281	291	312	333	303	325	295	317	285	318
1953	316	442	431	383	425	412	363	358	334	327	326	323
1954	333	305	301	300	310	342	313	297	307	292	329	294
1955	339	363	314	346	310	308	276	274	272	249	219	260
1956	293	383	402	357	356	335	323	306	295	280	263	247
1957	342	455	471	519	487	471	426	357	321	343	420	455
1958	463	410	355	395	381	377	354	285	311	292	298	311
1959	385	442	407	382	394	393	312	358	326	349	380	309
1960	354	354	312	323	317	352	351	329	309	299	333	316
1961	380	365	362	366	351	370	341	330	300	305	336	339
1962	371	336	319	377	369	386	355	327	352	314	295	286
1963	343	442	394	376	425	417	369	369	344	293	275	351
1964	322	373	356	286	299	291	309	282	297	264	279	274
1965	368	486	487	432	397	407	385	379	357	340	367	379
1966	395	342	310	343	336	337	345	344	310	317	291	292
1967	364	367	303	318	347	350	330	282	269	274	285	312
1968	328	313	317	338	344	379	421	369	320	306	374	327
1969	351	343	434	478	411	351	348	330	344	337	317	331
1970	334	278	328	341	281	328	292	307	299	322	273	226
1971	260	333	355	347	331	364	336	289	294	392	289	327
1972	412	501	461	427	436	505	463	367	374	384	445	539
1973	397	386	309	285	281	341	335	330	325	306	330	321
1974	254	284	376	400	396	431	427	333	318	332	341	343

Table 5. Monthly mean sea level (cm) at La Punta, Peru. Data courtesy of Dr. D. Enfield, Oregon State University.

Year	Jan	Feb	Mar	Apr	May	Jun	Jul	Aug	Sep	Oct	Nov	Dec
1950	212	212	239	246	258	261	228	225	185	181	197	197
1951	232	279	285	305	378	388	289	269	247	251	236	247
1952	265	265	254	284	296	275	256	251	215	234	218	244
1953	245	343	308	325	328	232	286	283	249	239	199	224
1954	221	220	226	226	242	256	212	200	195	178	239	202
1955	234	232	263	254	235	241	223	174	177	152	161	178
1956	222	264	262	269	246	252	204	229	202	178	190	175
1957	240	325	355	400	393	371	319	267	233	259	281	332
1958	383	341	280	291	290	297	283	216	202	207	229	245
1959	309	317	317	286	249	270	240	240	171	211	220	207
1960	223	253	196	237	223	266	219	221	195	219	219	223
1961	272	261	285	236	280	258	245	245	193	195	181	244
1962	270	241	248	290	241	273	268	244	236	193	208	188
1963	228	251	260	264	285	294	269	247	218	230	245	243
1964	217	234	222	208	224	221	241	196	181	178	165	182
1965	214	281	373	314	273	291	329	270	282	207	300	269
1966	270	227	213	239	233	264	257	212	198	214	193	207
1967	231	233	236	240	287	248	240	195	166	177	182	205
1968	216	207	240	240	221	267	282	237	245	254	220	222
1969	262	296	337	387	306	277	274	250	285	237	300	272
1970	312	309	283	278	331	328	246	236	231	226	205	218
1971	211	270	288	302	279	226	224	219	220	234	212	215
1972	237	287	350	317	381	402	379	318	319	287	354	421
1973	316	276	212	201	227	217	229	193	198	179	186	187
1974	230	202	268	276	295	301	290	275	236	322	325	319

real-time as BATHY messages for support of real-time ocean analyses. BATHY messages, although more timely, require additional editing to correct digitizing and transmission errors. With improved digital data acquisition and satellite data transmission systems, the time lags and transmission errors are being reduced.

Subsurface temperature profiles from many available sources have been assembled by FNOC in the Master Oceanographic Observations Data Set (MOODS). MOODS is in a compact binary format and contains almost 5 million subsurface temperature profiles globally. The MOODS file is by no means a complete file of all ocean temperature profiles that have even been made; rather, it is only that subset which have been made available to FNOC and merged into the file. Probably many additional profiles exist and if obtainable, could be used to improve analyses of historical conditions. At present, MOODS occupies 12 reels of magnetic tape and is sorted in the sequence: month, 1 degree square of latitude and longitude, year, day and hour. For compactness, many of the temperature profiles are stored at significant or inflection points so that the original data can be recreated by linear interpolation between inflection points.

The distribution of the profiles in time and space is critical for making consistent time series of subsurface temperature. A total for all years of only 12,102 profiles were available in the MOODS file for the five areas along the Peru coast (Fig. 3). Temperature profiles off Peru are almost nonexistent in the MOODS file for the years prior to 1955 but are more abundant for the years from the late 1950s to the early 1970s. Lags in data assimilation have reduced the amount of data in MOODS since the mid-to-late 1970s, with most of the recent data being acquired via BATHY messages. Profiles taken prior to 1952 have been included in the analysis by combination into the single composite year, labelled "1951" in the plots and tables. Inclusion of early profiles in the analysis is useful to help establish the edition scheme and to improve the long-term means.

In addition to an insufficient quantity of profiles over the 33-year analysis period, many of the available profiles are very "patchy" in their distribution. A cell in the data fields having 100 or more observations is often surrounded by many cells with no observations. This inhomogeneity of the data fields reflects the fact that relatively large numbers of temperature profiles are taken during short, localized research expeditions.

The subsurface temperature profiles in the MOODS file suffer from many types of errors. Teague et al. (1985) have described some of the errors based on samples of the data for the North Atlantic. Many of the profiles have erroneous spikes and tails which require editing, whereby the profiles are truncated to retain the portion of the profile above the erroneous data. About 1 to 5% of the profiles are from incorrect positions or times, as evidenced by reports from land areas. No attempt was made in this analysis to correct for position and time errors of the profiles as this would have required resorting the profiles into original cruise sequences and tracking each ship individually.

Because of the errors in profiles and more importantly insufficient distribution of observations in time and space, a complicated scheme was necessary to compute reasonable monthly mean values. Thus, the MOODS profiles were edited, monthly means were computed, and then the means were interpolated to fill gaps in coverage.

Editing Scheme for Subsurface Temperature Profiles

The first stage of editing the profiles was a gross error check requiring all reported temperatures to be in the range of -2.0 to +38.0°C and all depths to be nonnegative and increase sequentially. No two temperatures were allowed from the same reported depth; in such cases (which are rare), the depth of the second reported temperature was increased by an arbitrary value of 1 m. In order to eliminate gross error spikes, the size of allowable temperature changes between successive reported depth levels was limited between +2.0 and -12.0°C. When data were rejected by these edits, the profile was truncated at the depth of failure and the remaining upper portion of the profile was retained.

The second stage of profile editing checked for unusually strong positive and negative vertical temperature gradients to further reduce unreal spikes and vertical gradients. In the surface layer and thermocline, where the water temperatures were greater than 6.0°C, the

vertical temperature gradients were required to be in the range of -2.0 to +0.5ºC per meter of depth. For reported temperatures less than 6.0ºC, the allowable gradients were tightened to -0.5 to +0.1ºC/m. As for the first stage editing, when gradients exceeding these limits were encountered, the profiles were truncated and the remaining, upper portions of the profiles were retained.

The third stage of editing was a check against the mean and standard deviations of a running series of 10 values of a temperature editing parameter. For SST, depths of the 14ºC and SST-2ºC isotherms and heat content, the computed parameter itself was used as the editing parameter. For the vertical temperature series, the temperature at 100 m was interpolated from each profile and used as the editing parameter. The running series was started with the first 10 profiles for each month and 1 degree square of latitude and longitude. (Because the data were sorted in the sequence: month, 1 degree square, year, day and hour, the first 10 profiles in a one degree square were often from years earlier than 1952 and thus errors in the first 10 profiles did not cause serious contamination of the 1952-1984 time series). After acceptance of the first 10 profiles, the mean and standard deviation of the running series of 10 editing values were computed and used to check the next profile. A new profile was accepted if the editing parameter computed from it was within a specified tolerance of the mean of the previous 10 values, where the tolerance was arbitrarily defined to be 1.3 times the standard deviation of the previous 10 values. Each new accepted value was then added to the series and the oldest value in the series deleted. Use of the running series of 10 values allowed the editing mean to move up or down with warm and cold periods defined by the data themselves. Similarly, the scheme allowed the editing tolerance range to widen as the data became more variable (in periods of climatic change or in areas near oceanic boundaries) and to narrow as the data became less variable (during more stable periods or in areas far from oceanic boundaries).

Computation of Individual Monthly Mean Values

After editing the temperature profiles as described above, values of the four parameters (SST, depth of the 14ºC isotherm, depth of the SST-2ºC isotherm, and heat content down to the SST-2ºC isotherm were computed for each profile. Individual monthly means of the four parameters were computed for each cell (5 areas x 408 months) for the years 1951 to 1984. The resulting monthly mean fields were very sparse, having mean values in only about 37% of the 2,040 total cells.

Temperatures at 25 m depth intervals from the surface to 350 m were computed from each profile to display vertical variations of temperature versus time in each of the five areas. The data were processed as differences between the surface temperature and the temperature at each 25 m depth interval because of the effect of varying maximum depths of the profiles. Direct computation of mean temperatures from profiles of varying maximum depth can cause unrealistic subsurface temperature gradients (Robinson and Bauer 1976).

After computation of the individual monthly mean values, the 12 long-term monthly means and 12 between-year standard deviations were computed for each area (or depth for the vertical plots). Here, long-term mean is defined as the mean of all the individual monthly means, e.g., the January long-term mean is the mean of all individual January monthly means. The between-year standard deviation (bysd) is the standard deviation of the individual monthly means computed by month to show the interannual variability. The monthly anomalies were then computed as the differences between the individual monthly means and the appropriate long-term monthly mean, e.g., the January 1952 anomaly is the individual monthly mean for January 1952 minus the January long-term mean.

In some cases, no profiles were available in a month during any year for an area (or depth). In these cases, it was not possible to compute a long-term monthly mean. Such gaps in the long-term mean field were filled using a 5 x 5 matrix interpolation which used information from surrounding long-term means. Empty cells were filled with averages of surrounding mean values, weighing proportionately to the square root of the number of years of data represented by the mean and inversely to the square of the distance (in grid lengths) away from the cell.

The fields of individual monthly mean values were rather noisy, particularly those computed from small numbers of profiles which are considered less reliable than those based on relatively large numbers of profiles. To reduce the errors associated with limited numbers of profiles, the individual monthly means were adjusted toward the long-term mean for each month, i.e., means based on only a single profile were set to the average of the mean and the long-term mean for that month, while means based on two or three profiles were weighed proportionately less toward the long-term mean.

Monthly anomalies were computed as the difference of the adjusted individual and long-term monthly means. To partially fill the gaps in the anomaly field between data values, the same 5 x 5 matrix interpolation scheme was used as for the long-term means, weighing proportionately with the square root of the number of profiles represented by the mean and inversely with the square of the distance away from the cell. In regions that were 3 or more cells away from mean values, no interpolation of the anomaly was made. Use of this interpolation scheme increased coverage of the field from about 37% to about 91%. Use of a 5 x 5 matrix interpolator was reasonable as autocorrelation functions (not shown) of the individual monthly means were computed and had magnitudes greater than 0.4 for lags of at least two months in time and at least three areas (9 degrees of latitude) along the coast in space. The correlations are in agreement with Enfield and Allen (1980) who showed similar strong coastwise coherence of sea level and SST along the coast of North and South America from Alaska to Chile.

After adjustment and interpolation of the anomaly field, the fields of individual monthly means were recomputed. Gaps in the coverage were partially filled by the addition of the interpolated anomaly field and the long-term mean field. Use of the anomaly fields to interpolate the monthly mean fields for filling gaps in coverage is based on the assumption that the anomaly fields are smoother in time and space than the monthly means. This assumption is justified because of the large seasonal changes that are observed in the monthly means but relatively smoother changes in the anomalies (see, e.g., Fig. 2, autocorrelation functions).

Spatially Averaged Monthly Means for the 4 to 14°S Region

Monthly anomalies for the three central areas were further averaged to make time series of monthly mean anomalies for the entire region from 4 to 14°S. The averaged monthly anomalies were then added to the appropriate averaged long-term means to obtain time series for the four computed parameters by month for the region 4-14°S. Plots and tables of the time series values are presented along with the total combined number of observations for the three central areas. Values are only given if observed or interpolated mean values were available for all three areas. This requirement reduced the coverage of the time series to about 90% of the 408 possible months. For cases where anomaly values were not available for each of the three areas for any particular month, asterisks are printed in the tables and values are not plotted.

Results and Discussion

Each of the parameters (SOI, SST, sea level, depth of the 14°C isotherm, depth of the SST-2°C isotherm, vertical structure of subsurface temperature and heat content from the surface to the SST-2°C isotherm) is presented separately. The data are displayed in a variety of formats to emphasize the seasonal and interannual scales of variability, both horizontally along the coast and vertically through the water column. For each of the parameters, tables and plots of spatially-averaged (for the region from 4-14°S) monthly means are presented. Plots of the long-term annual cycle, between-year standard deviation, monthly anomaly in standard deviation units, and autocorrelation functions of the anomalies for each of the parameters are presented to describe seasonal and interannual variability. Also, time-latitude and time-depth contour plots of profile data are presented to show horizontal and vertical variations of subsurface temperature.

Southern Oscillation Index

Time series of the monthly mean Southern Oscillation Index (Fig. 1A, Table 1) and anomaly of SOI (Fig. 2A) show the buildups and subsequent declines of pressure differences associated with the onset of El Niño, as described earlier. Major buildups and declines occurred in 1949-1952, 1954-1958, 1970-1972 and 1975-1977. The most recent decline in 1982-1983, associated with that strong El Niño, followed a long period (1976-1981) of relatively weak negative pressure difference. There was also a sharp decline in 1979 associated with a weak coastal warming event in that year. Perhaps the 1979 event would have been more notable (more comparable to other moderate or weak El Niños) if it had not occurred during an already warm period.

The SOI has a relatively strong annual cycle (Figs. 1 and 2) which varies from a peak difference of about 13 mbs in February, indicating strongest trade winds in late austral summer to a low of about 7 mbs in May, indicating weakest trade winds in late austral fall. The interannual variability of SOI is relatively constant throughout the year as indicated by the similar values of between-year range and standard deviation. The SOI is moderately persistent in time with an autocorrelation of anomaly of about 0.4 at one month lag. From 12 to 36 months lag, the autocorrelation of the anomaly remains very close to zero, then becomes weakly positive at lags of 36-48 months. This suggests that the period of important interannual changes in the SOI is greater than 3 years, in agreement with the frequently reported period for El Niño of 3-7 years.

Sea Surface Temperature

Time series of monthly mean SST (Figs. 1B and 1C, Tables 2 and 3) and anomaly of SST (Figs. 2B and 2C) at Talara and La Punta (Callao) and spatially-averaged SST for the region from 4-14°S (Table 6, Figs. 4A, 5A) show significant seasonal and interannual variability of SST. Both the shore station and spatially-averaged SST data show the major El Niño and anti-El Niño events. Positive anomalies occurred in the years 1953, 1957-1958, 1965, 1972-1973, 1976-1977, 1979 and 1982-1983. Each of the figures also show longer period interannual variations: cool conditions in the early 1950s, warm conditions in the late 1950s, moderately cool conditions throughout the 1960s and early 1970s (except the 1965 and 1972-1973 El Niños), and finally a long-term warming during 1976-1983. Comparison between the two shore stations, Talara in the north and La Punta in the south, shows the northerly station to have more low-amplitude, high frequency variability than the southerly station. This difference is assumed to be caused by the more complicated equatorial ocean dynamics occurring in the northern region.

Along the coast, the El Niño events of 1953, 1957-1958, 1965, 1969, 1972-1973, 1976-1977 and 1982-1983 (Rasmusson 1984) are seen as tongues of warm SST, extending variable distances southward (Fig. 6). A moderate warming occurred in 1979-1980, in agreement with the below normal SOI that year. The extreme magnitude (large region of SST > 28°C), duration, and coastwise coherence of the 1982-1983 event distinguish it as the most significant warm feature of this series. The poorly documented 1953 El Niño shows a surprisingly strong surface manifestation of warm water. The 1954-1956 cold event is only weakly evident, probably due to sparse data. With the exception of the 1982-1983 warm event, each of the warm surface events are shown to be preceded by a period of anomalously cool SST.

The annual cycles of SST at the two shore stations (Figs. 2B and 2C) and for the spatially-averaged region (Fig. 7A) vary from highs during the austral fall to lows during the austral spring. The amplitude of the annual variation of SST is greatest nearer to the equator and the complex dynamics associated with the interaction of equatorially-trapped waves with the eastern boundary (Fig. 6). The spatially-averaged long-term means (Fig. 7A) show high SST (>23.5°C) from January through March or April, when warm water intrudes from the north, followed by a rapid transition to lower temperatures in April with the onset of upwelling along the central and southern portions of the coast. SSTs of 17-19°C occur during the upwelling regime from May to October along the coast, except for the northernmost area where upwelling is weak.

Along the coast, the annual cycle is strong, varying between upwelling and nonupwelling regimes for the central and southern areas and the weak seasonal variation for the northern area.

Table 6. Monthly mean surface temperature (C) for the region 4-14° off Peru. These means are averages of the monthly means for the three Central areas, computed from subsurface temperature profiles. The corresponding number of profiles used in computing each mean is printed (in brackets) to the right of the mean. Means based on zero profiles are computed from interpolated values. Asterisks indicate months in which neither observed nor interpolated means were available in all three areas.

| Year	Jan	Feb	Mar	Apr	May	Jun	Jul	Aug	Sep	Oct	Nov	Dec
1951	23.0 (1)	24.3 (1)	24.5 (129)	23.5 (0)	19.5 (0)	18.2 (2)	18.5 (36)	17.6 (6)	16.8 (0)	17.6 (0)	19.2 (0)	21.0 (0)
1952	22.8 (35)	23.9 (0)	23.6 (0)	**** (0)	17.5 (0)	17.3 (0)	17.4 (129)	16.2 (0)	16.8 (0)	17.6 (0)	19.2 (0)	21.0 (0)
1953	24.4 (0)	25.2 (0)	25.1 (49)	23.1 (93)	19.8 (23)	19.8 (0)	19.7 (0)	**** (0)	**** (0)	**** (0)	**** (0)	**** (0)
1954	**** (0)	**** (0)	*/** (0)	**** (0)	**** (0)	**** (0)	17.3 (0)	16.3 (2)	15.5 (0)	**** (0)	**** (0)	**** (0)
1955	**** (0)	**** (0)	**** (0)	**** (0)	**** (0)	**** (0)	**** (0)	**** (0)	16.8 (0)	17.2 (0)	**** (0)	**** (0)
1956	21.0 (5)	22.5 (0)	22.8 (0)	22.0 (31)	18.5 (0)	18.4 (0)	19.5 (0)	18.5 (0)	17.8 (31)	18.3 (0)	19.3 (51)	19.7 (95)
1957	23.9 (0)	24.8 (1)	26.1 (33)	23.3 (25)	20.6 (0)	20.1 (0)	**** (0)	**** (0)	17.0 (0)	18.3 (0)	19.9 (13)	21.5 (0)
1958	23.1 (75)	24.5 (10)	24.1 (66)	22.8 (8)	19.6 (4)	19.0 (0)	**** (0)	18.6 (7)	17.2 (0)	17.6 (0)	18.8 (15)	21.3 (6)
1959	22.7 (0)	23.9 (0)	23.8 (32)	22.6 (0)	19.2 (0)	**** (0)	**** (0)	18.0 (0)	17.2 (0)	17.9 (4)	18.6 (5)	21.0 (160)
1960	21.4 (0)	22.8 (4)	21.6 (13)	22.3 (51)	18.5 (4)	19.0 (0)	18.7 (0)	17.3 (0)	16.5 (14)	16.8 (97)	19.4 (0)	20.5 (0)
1961	21.5 (0)	22.7 (79)	21.5 (63)	20.2 (60)	17.0 (0)	17.9 (14)	17.7 (9)	17.0 (156)	16.8 (29)	17.5 (8)	19.0 (1)	20.1 (0)
1962	21.4 (93)	21.2 (89)	21.4 (24)	20.8 (98)	18.3 (94)	18.1 (37)	17.7 (47)	16.9 (0)	16.1 (0)	16.9 (18)	18.1 (41)	20.1 (0)
1963	21.6 (33)	22.9 (178)	22.2 (55)	20.7 (69)	17.8 (0)	18.3 (0)	17.9 (55)	18.2 (142)	17.6 (46)	16.6 (155)	17.8 (274)	20.1 (61)
1964	21.7 (0)	23.1 (10)	21.5 (38)	21.5 (0)	18.5 (42)	18.0 (65)	18.0 (3)	16.4 (47)	15.9 (49)	16.0 (8)	18.8 (44)	19.9 (72)
1965	22.6 (0)	24.9 (10)	23.8 (1)	24.1 (43)	20.4 (0)	19.9 (0)	19.9 (31)	18.6 (66)	18.0 (49)	17.7 (26)	18.6 (175)	20.6 (2)
1966	22.2 (0)	23.0 (80)	22.5 (57)	22.0 (17)	18.5 (50)	17.7 (9)	18.5 (0)	17.5 (5)	16.8 (148)	16.9 (2)	19.4 (135)	21.5 (15)
1967	21.8 (0)	22.7 (116)	23.8 (15)	21.4 (5)	18.5 (45)	18.6 (2)	17.8 (2)	16.6 (95)	16.1 (69)	16.5 (0)	18.7 (28)	20.0 (49)
1968	21.3 (0)	22.9 (97)	22.2 (0)	20.8 (2)	16.1 (55)	16.0 (0)	18.1 (0)	18.0 (0)	17.6 (86)	17.4 (38)	18.3 (28)	18.9 (48)
1969	22.4 (46)	23.3 (20)	23.7 (8)	23.0 (2)	18.9 (0)	19.2 (8)	18.7 (53)	17.8 (36)	17.2 (159)	17.5 (0)	18.1 (12)	20.3 (71)
1970	21.9 (0)	22.8 (0)	21.4 (0)	20.3 (0)	17.1 (8)	17.0 (33)	17.5 (0)	16.8 (0)	16.1 (63)	16.7 (94)	18.9 (62)	20.2 (19)
1971	20.6 (0)	21.8 (0)	22.2 (0)	20.3 (5)	18.9 (23)	19.3 (19)	18.4 (0)	17.2 (151)	16.5 (43)	16.3 (11)	17.0 (100)	18.3 (32)
1972	22.4 (1)	24.3 (19)	24.7 (68)	23.3 (68)	20.8 (14)	20.5 (1)	20.7 (31)	19.5 (0)	18.2 (0)	18.2 (20)	18.4 (109)	19.6 (62)
1973	23.7 (0)	24.6 (16)	22.6 (89)	20.6 (6)	18.1 (2)	17.4 (0)	17.8 (6)	16.3 (33)	16.5 (25)	17.1 (1)	20.6 (139)	22.1 (4)
1974	22.2 (2)	20.5 (28)	21.7 (38)	21.2 (5)	19.0 (4)	19.4 (34)	18.9 (3)	17.7 (6)	16.7 (0)	17.4 (3)	18.9 (0)	19.3 (0)
1975	22.5 (6)	23.7 (2)	23.8 (53)	22.5 (29)	19.6 (37)	18.8 (1)	18.1 (0)	16.8 (133)	15.9 (0)	16.3 (0)	18.6 (65)	20.5 (0)
1976	21.6 (0)	23.3 (0)	23.3 (4)	22.0 (21)	19.1 (0)	19.8 (0)	20.3 (25)	18.3 (26)	17.9 (0)	19.2 (16)	17.6 (13)	20.0 (17)
1977	23.6 (0)	25.0 (26)	24.7 (0)	23.5 (1)	19.5 (0)	19.0 (9)	18.9 (0)	17.6 (13)	17.3 (0)	18.4 (11)	20.2 (0)	21.6 (27)
1978	22.0 (0)	22.9 (0)	22.6 (5)	22.1 (0)	19.7 (1)	18.7 (0)	18.3 (9)	17.4 (0)	17.2 (0)	18.3 (0)	19.0 (11)	20.8 (0)
1979	23.2 (0)	**** (0)	**** (0)	**** (0)	**** (0)	19.8 (0)	19.8 (0)	18.8 (28)	18.1 (0)	18.5 (0)	19.9 (19)	21.5 (0)
1980	23.4 (0)	24.9 (4)	24.7 (11)	23.7 (0)	20.0 (0)	19.3 (0)	19.3 (0)	18.4 (12)	17.6 (0)	18.2 (0)	19.5 (0)	21.1 (8)
1981	23.0 (0)	24.1 (0)	23.6 (21)	2.8 (0)	19.5 (0)	**** (0)	**** (0)	**** (0)	17.1 (0)	17.8 (0)	**** (0)	**** (0)
1982	22.4 (0)	22.8 (1)	21.5 (29)	22.4 (21)	18.9 (0)	19.6 (0)	19.6 (0)	18.6 (19)	18.5 (0)	20.5 (0)	19.2 (34)	21.4 (19)
1983	26.0 (0)	27.4 (17)	26.5 (1)	26.0 (31)	22.5 (0)	22.4 (30)	21.5 (18)	19.0 (2)	18.3 (0)	19.1 (11)	22.6 (34)	23.4 (6)
1984	24.1 (0)	25.3 (12)	25.0 (0)	23.7 (0)	19.0 (0)	19.0 (0)	18.8 (11)	18.2 (12)	17.4 (0)	17.9 (0)	19.4 (7)	**** (0)
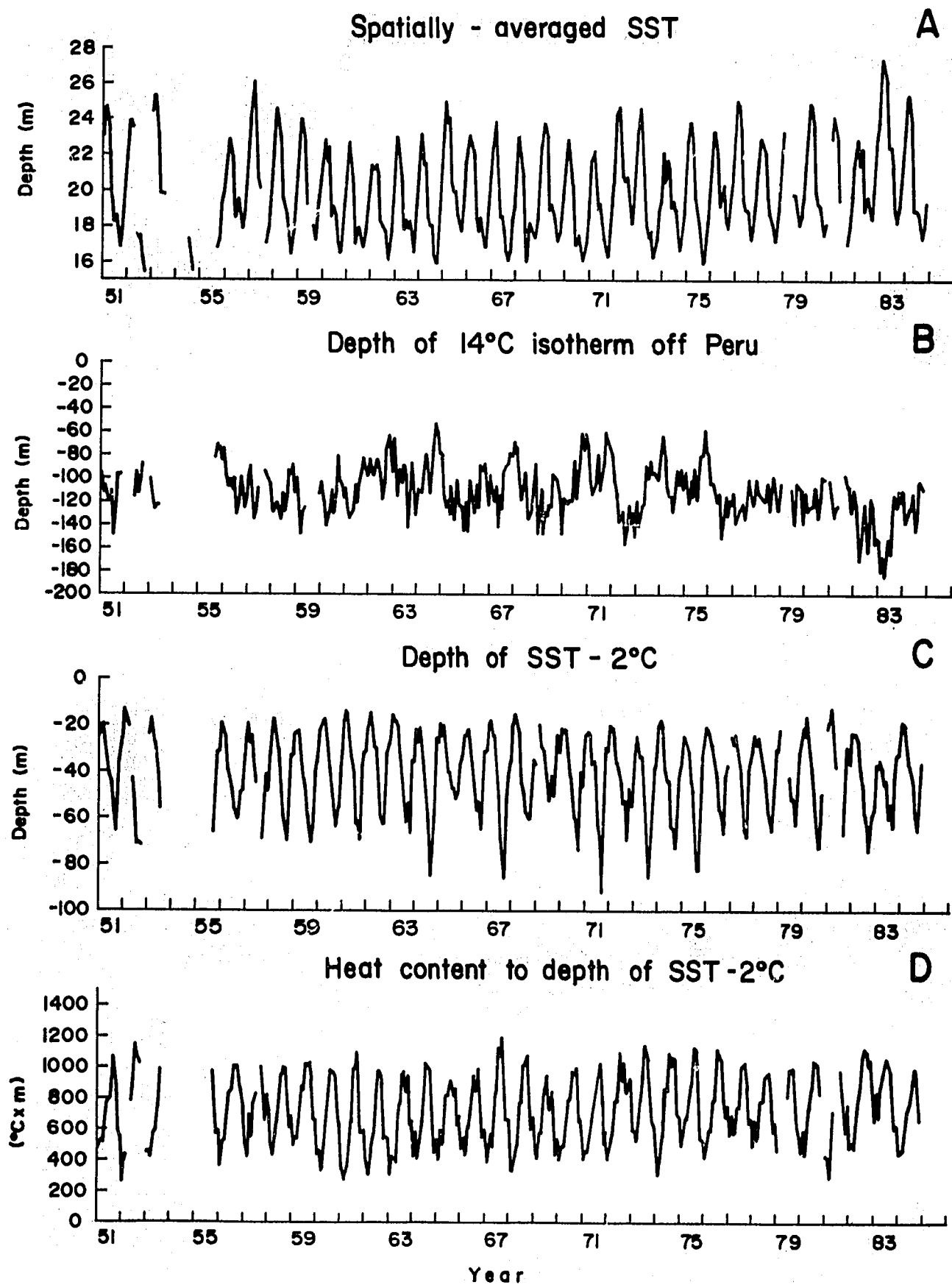
Fig. 4. Time series of spatially-averaged monthly means for the region 4 to 14°S as computed from profiles of subsurface temperature. Parameters are (A) SST, (B) depth to 14°C isotherm, (C) depth to SST-2°C isotherm, and (D) heat content from the surface down to SST-2°C.
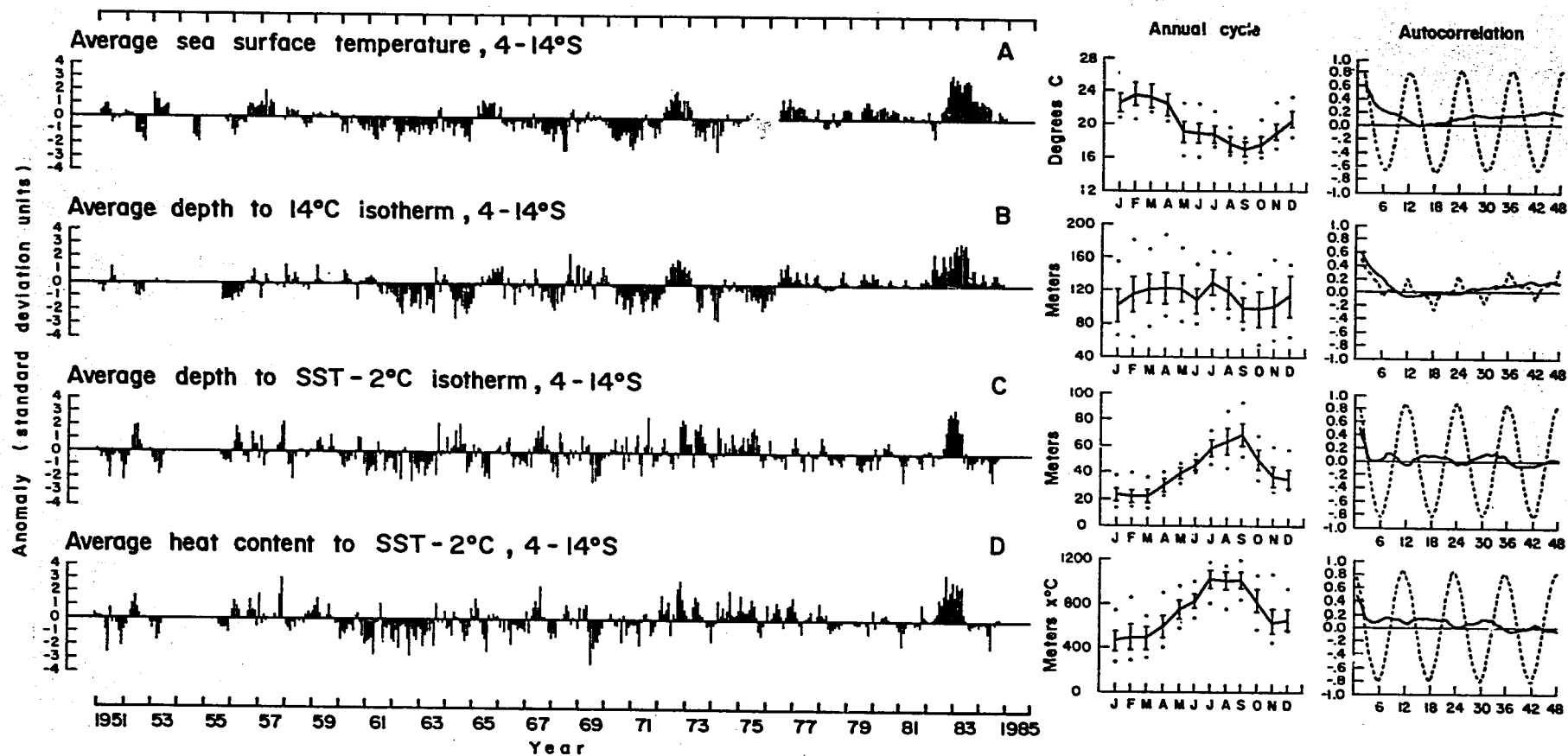
Fig. 5. Annual cycles, autocorrelation functions, and anomalies of (A) SST, (B) depth of the 14°C isotherm, (C) depth of SST-2°C isotherm, and (D) heat content from the surface down to SST-2°C isotherm off Peru from 1952 to 1984. Data shown for "1951" are a composite of data for all years prior to 1952.
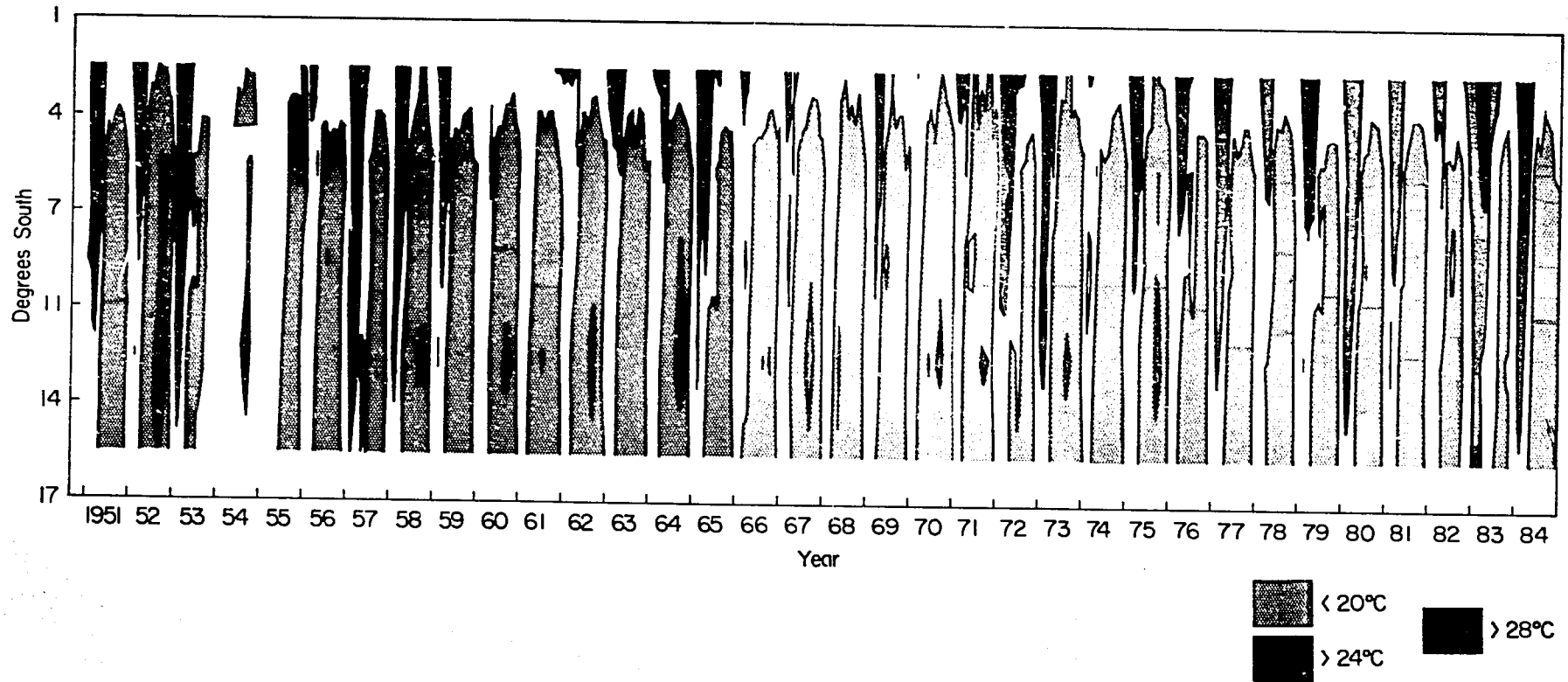
Fig. 6. Time-latitude contour plot of monthly mean SST for the 5 areas off Peru. Data shown for "1951" are a composite of data for all years prior to 1952. Tongues of water greater than 24°C penetrate a variable distance southward along the coast during January to March from year to year and are indicators of El Niño. Water of greater than 28°C intruded southward in early 1983. Low temperature tongues, associated with upwelling, extend northward.

A. SST

☐	0-17.5	☐	0-0.9
▦	17.5-19.9	▦	1.0-1.9
▦	20.0	■	>2.0
▦	20.1-23.5		
■	>23.6		

B. Depth of 14°C isotherm

▥	0-99.9m	☐	0-23.9m
▦	100-150m	▦	24.0-49.9m
■	>150m	■	)50.0m

C. Depth of SST - 2°C isotherm

☐	0- 19m	☐	0-11.9m
▦	20- 49m	▦	12-21.9m
▦	50- 74m	■	>22m
▦	75-100m		
■	)100m		

D. Heat content down to SST - 2°C isotherm

▦	0- 499	☐	0- 99
▦	500- 749	▦	100-249
▦	750- 999	■	>250
■	1,000-1,249		
■	>1,250		

Degrees South

Month
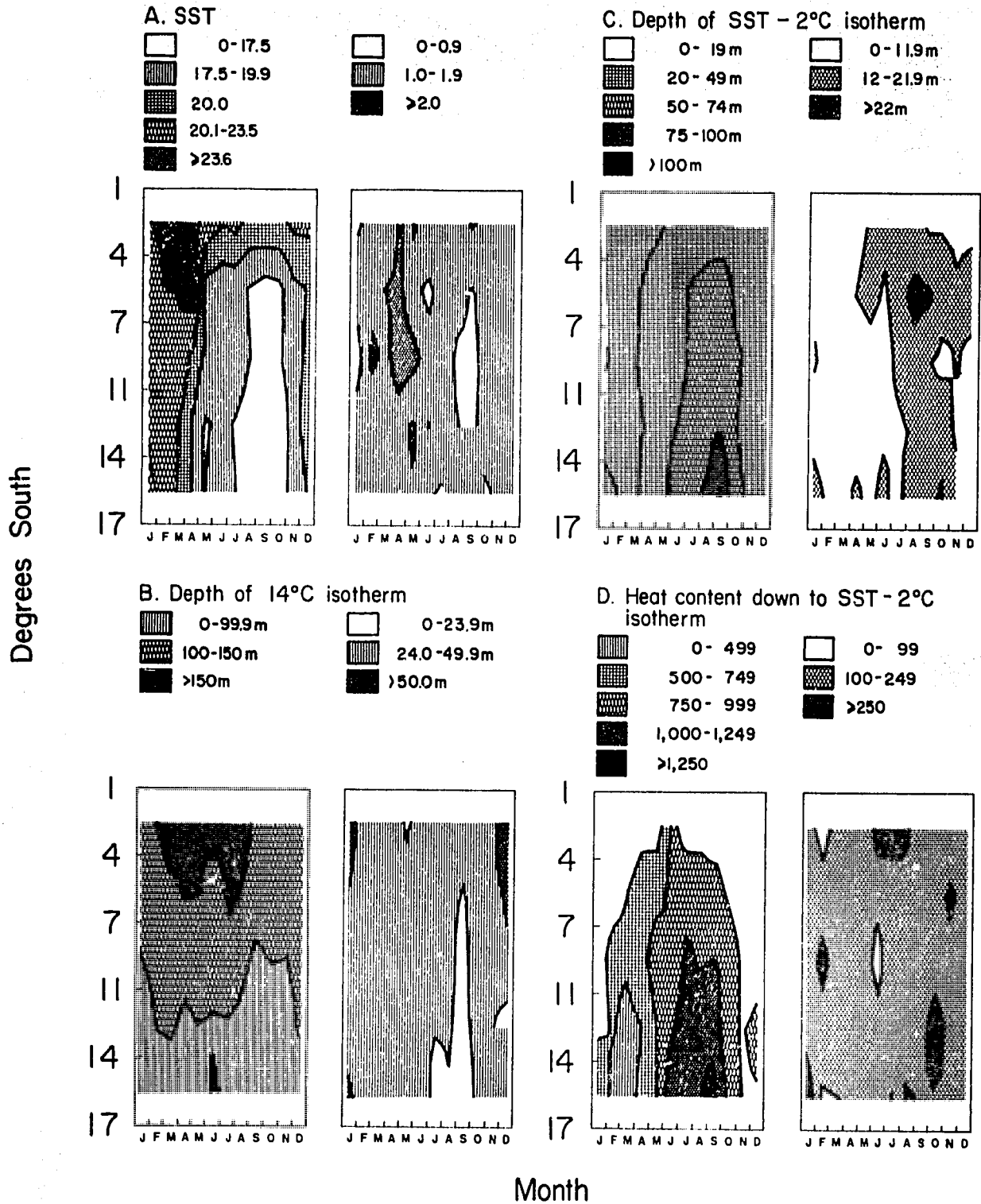
Fig. 7. Time-latitude contour plots of annual cycles and between-year standard deviations of (A) SST, (B) depth of 14°C isotherm, (C) depth of SST-2°C isotherm, and (D) heat content down to SST-2°C isotherm for 5 areas along the Peru coast. The long-term mean annual cycles are shown in the left-hand plots. When no profiles were available for a month in any year, the long-term mean was interpolated. The between-year standard deviations are shown in the right-hand boxes.

The time-latitude between-year standard deviation plot (Fig. 7A, left-hand plot) shows the highest interannual variability to occur during the fall transition from the warm current regime to the upwelling regime, particularly in area 2 which is between the strong upwelling to the south and the weak upwelling to the north. The interannual variability of SST is lowest during peak upwelling.

The autocorrelation function of the anomaly of the spatially-averaged SST (Fig. 5A) is moderately persistent with a lag one value of about 0.6. After 18 months' lag, the autocorrelation function begins to rise, peaking again at a lag of about 44 months. Anomaly of SST at the two shore stations has autocorrelation functions with moderately strong persistence at lags one and two, negative correlation between lags of 12 and 36 months, and weakly positive correlation after a lag of about 40 months (see Figs. 2B, 2C). This pattern is similar to that described for SOI.

Vertical Structure of Subsurface Temperature, 0-350 m

The interannual variability of subsurface temperature for the central area (Area III) off Peru (Fig. 8) shows monthly variations of isotherm depths from the surface to 350 m for the period 1952 to 1984. A similar plot of the anomaly field was used for the analysis (but not shown because anomalies must be carefully analyzed to avoid misinterpretation of events caused by slight phase shifts). Interestingly, the 12, 14 and 16°C isotherms show a general long-term depression of the thermal structure for the period 1976-1984, in agreement with the changes in SOI and SST discussed previously and with other reports of a large-scale coastal warming during the period.

Shorter duration depressions of the isotherms are observed for the 1957-1958, 1965-1966, 1969, 1972-1973, 1976-1977, 1979-1980 and 1982-1983 El Niño warming events. The magnitude and vertical extent of these isotherm depressions varies noticeably between different events. Each of these El Niño events is characterized by moderate to strong surface warming. The anomaly field (not shown) has double peaks for most of these warming events, as has been reported by others for many El Niño events (e.g., Cane 1983; Reinecker and Mooers 1986). The 1957-1958 El Niño appears to be of shallower extent but of longer duration than most of the other events, lasting for about 3 years. The 1965-1966 El Niño had intense surface warming (down to 150 m) which began in January 1965 and lasted until about July, followed by a second, weaker warming which peaked in about December. There was also a weak isotherm depression between 275 and 350 m. The 1969 El Niño had a weak signal from the surface down to about 300 m. The 1972-1973 El Niño was similar in vertical extent and duration to the 1965 event, except the second peak was less defined. The 1976-1977 event was moderately strong at all depths from the surface down to 350 m. The 1979-1980 event had a weak depression at all depths. During the 1982-1983 El Niño, a strong depression of 50 to 80 m was observed at all depths. For this event, it is interesting to note that the 12 and 14°C isotherms were depressed 5-6 months prior to the depressions of the surface layer isotherms. It is yet to be determined whether this relates to the idea of downward and poleward propagating coastally trapped waves (McCreary 1976).

The annual cycles of subsurface temperatures for the five areas along the coast are shown by vertical contour plots of the long-term monthly means (Fig. 9). The areas are arranged from north to south from left to right across the page. The strongest vertical temperature gradients are in the upper 75 m, indicating a relatively shallow mean thermocline. The isotherms display a relatively linear slope upwards with increasing latitude (southward) along the coast, as would be expected. The 12 and 14°C isotherms shoal from mean depths of about 285 m and 170 m for Area I, near the equator, to mean depths of 205 m and 90 m for Area V, in the south. Similarly, the SST varies between 21 and 24°C for the northern area and between 16 to 21°C for the southern area. Each of these plots show a strong annual cycle having relatively warm temperatures during the austral summer, with annual highs occurring in February and March, and cooler temperature during the austral winter, with annual lows occurring in September. This pattern of the annual cycle becomes less apparent with increasing depth, where the 12, 14 and 16°C isotherms have an interesting double peak.

The interannual variability of subsurface temperature off Peru is shown by vertical contour plots of the between-year standard deviation (bysd, see Fig. 10) for the long-term monthly means
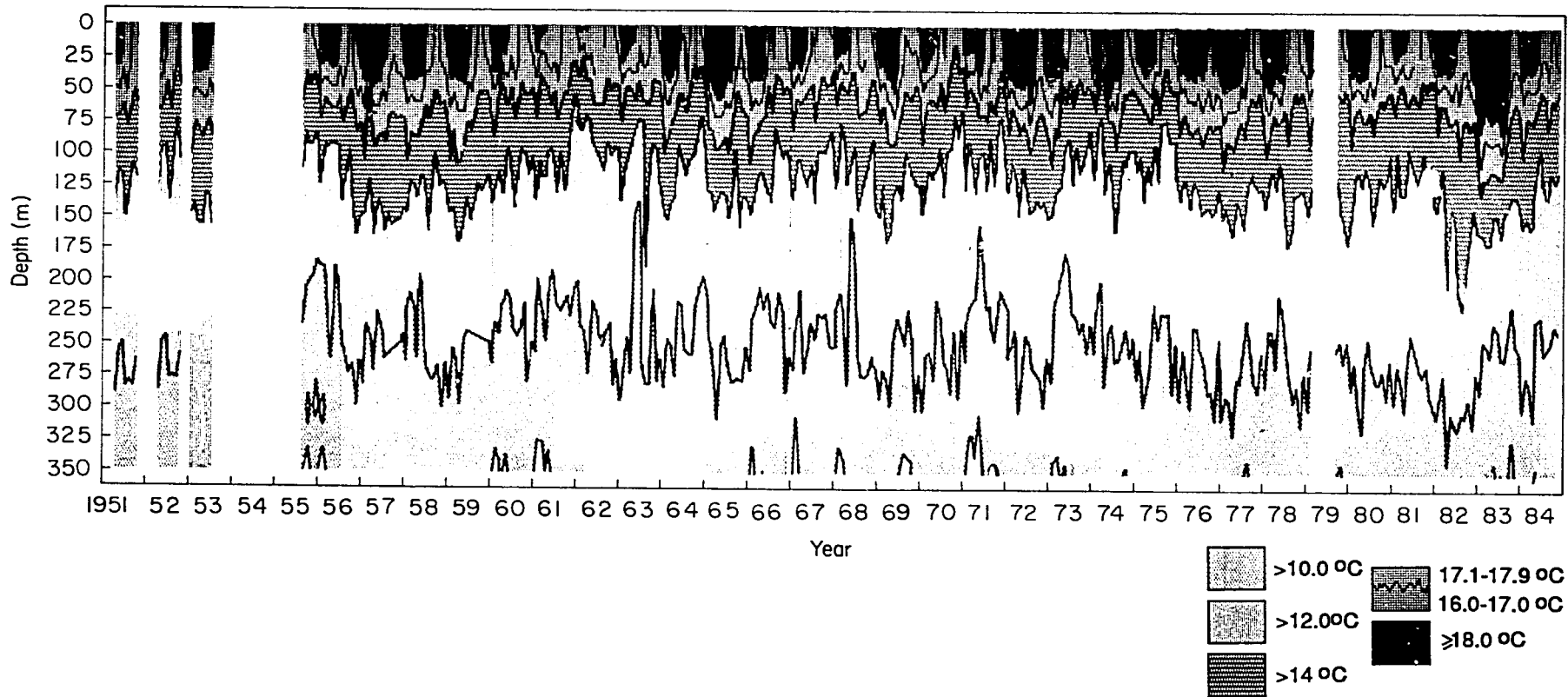
Fig. 8. Time-depth contour plot of monthly mean subsurface temperature off Peru from 1952 to 1984. Data are computed at 25 m depth intervals from 0 to 350 m from subsurface temperature profiles for central area (Area III). Values shown for "1951" are a composite of data for all years prior to 1952. Note the depression of the 12°C and 14°C isotherms from the early to mid-1970s to a maximum depth in 1982.
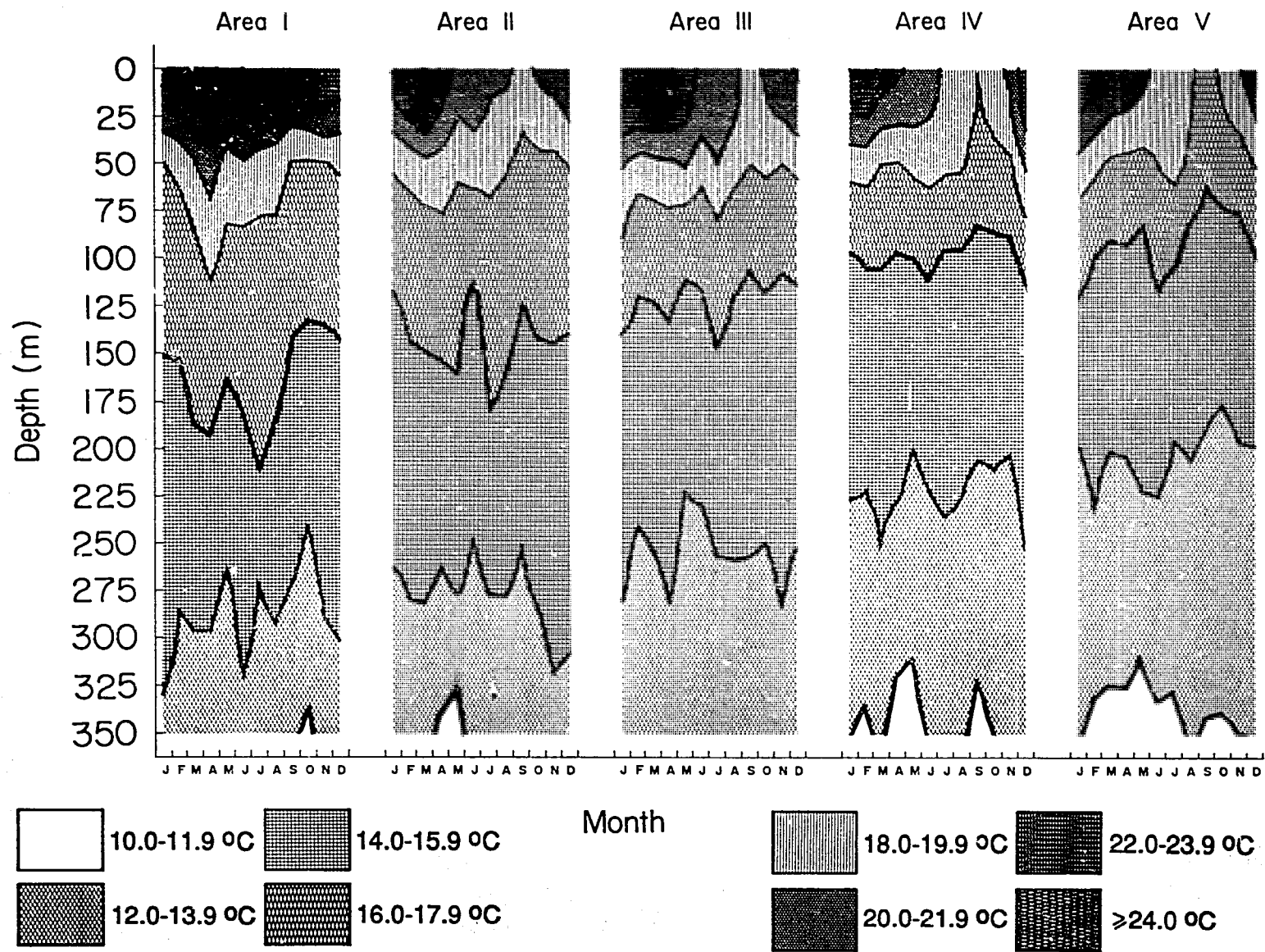
Fig. 9. Annual cycles of subsurface temperature vertically from 0 to 350 m for 5 areas along the Peru coast. Note the progressive rise of the isotherms from north (Area I on the left) to south (Area V on the right). For example, the 14°C isotherm rises from depths of 250-325 m in the north to depths of 75-125 m in the south.
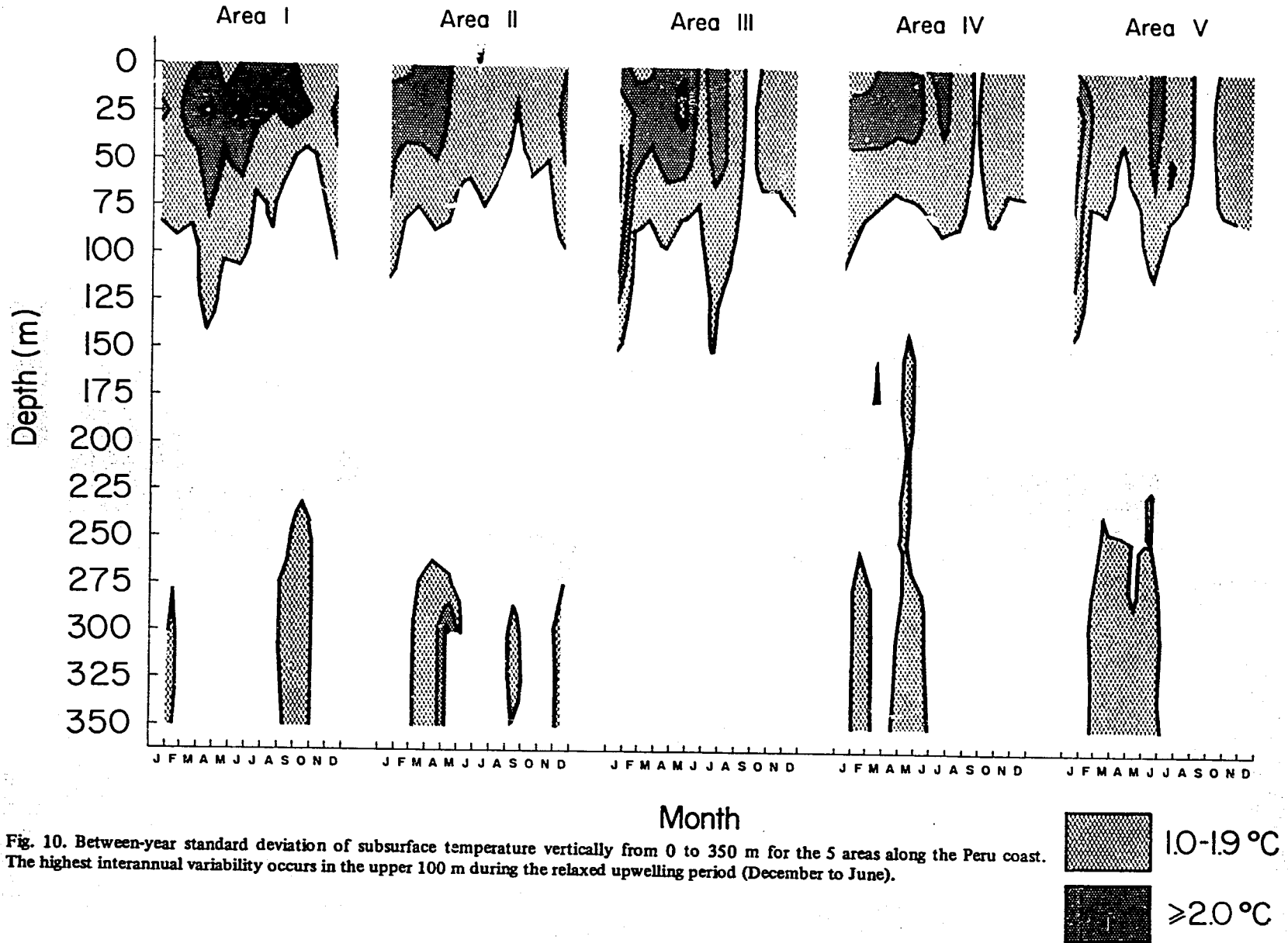
Fig. 10. Between-year standard deviation of subsurface temperature vertically from 0 to 350 m for the 5 areas along the Peru coast. The highest interannual variability occurs in the upper 100 m during the relaxed upwelling period (December to June).

just discussed. The highest variability is found in the upper 50 m, as would be expected for the thermocline. Seasonally, this upper layer variability appears to be highest (bysd = 2.7-3.0°C) from March through July and lowest (bysd = 0.7-1.2°C) in September. With a few exceptions, the interannual variability is consistently low (bysd = 0.2-0.9°C) below 100 m in each of the 5 areas.

Depth of the 14°C Isotherm

Unlike the previous section which described time variations of the thermal structure vertically for a single area and the long-term annual cycle of the slope of the thermal structure for the five areas along the coast, this section examines temporal and spatial variations of the depth of the 14°C isotherm in greater detail. The time series of monthly mean depth of the 14°C isotherm (Fig. 11, Table 7) shows considerable seasonal and interannual variability. The 14°C isotherm deepened during each of the warming events, with the most striking example occurring during the 1982-1983 El Niño. The anomaly of the depth of the 14°C isotherm (Fig. 5B) shows persistent deep or shallow anomalies lasting several years. The 14°C isotherm deepened in 1976 and remained anomalously deep throughout the rest of the record.

The annual cycle of the depth of the 14°C isotherm (Fig. 7B) differs from the annual cycles of each of the other parameters in that it displays a double peak. Seasonally, the depth of the 14°C isotherm for the region from 4 to 14°S has maximum depths in April and July and minimum depths in June and September. This double peak exists for each of the five areas (Fig. 9), although the months of occurrence differ slightly.

The 14°C isotherm is relatively deep in the north and shallow in the south (Figs. 9 and 11). The annual long-term mean depths of the 14°C isotherm for Areas I through V are 152, 135, 109, 99, and 78 m, respectively. The transition from depth to shallow depths is usually rapid, typically occurring in 1-2 months. The interannual variability of the depth of the 14°C isotherm is highest in December and January for the three northern areas (between-year standard deviations greater than 50 m), associated with the intrusion of the warm water. The interannual variability is lowest during peak upwelling in September.

Along the coast, the depth of the 14°C isotherm (Fig. 11) provides an indication of the coastwise interannual variability of the thermocline depth and the effect of coastal upwelling on the thermal structure. The 14°C isotherm deepened moderately during the years 1957-1958, 1965, 1969, 1976-1977 and 1979-1980 and strongly during the 1972-1973 and 1982-1983 El Niños. This plot shows the 1982-1983 El Niño to be the largest event of the record, both in magnitude and duration. The 14°C isotherm remained below 200 m for most of the period from February 1982 through July 1983 for the northern two areas. Likewise, the 14°C isotherm remained significantly deeper than normal during this period for the southern three areas. Both plots show the 1957-1958, 1965, 1969, 1972-1973 and 1976-1977 El Niños were preceded by cold period having shallow depths of the 14°C isotherm. The 1979-1980 and 1982-1983 warm events, by contrast, occurred during the long-term coastal warming from 1976 to 1984.

The 1979-1980 warming, which was not included in Rasmusson's (1984) list of El Niños, had moderate signals for each of the three parameters thus far discussed. Norton et al. (1984) described a strong surface warming in 1979-80 in the California current system which attenuated rapidly with depth, seemingly unrelated to tropical warming.

Wyrtki (1975) pointed out that El Niño conditions off the coast of Peru were not caused by a local weakening of the upwelling favorable winds, as had been previously hypothesized. He showed that not only did the upwelling favorable winds not weaken but also appeared to have strengthened during El Niño events. Using Bakun's (this vol.) time series of wind stress, turbulent mixing index, and offshore Ekman velocity and transport, we now strengthen Wyrtki's argument and show that each of the major El Niño events of the past three decades occurred during periods of anomalously strong southeast trades and offshore Ekman transport. One would expect intense offshore transport to be associated with intense coastal upwelling and shallow thermocline. However, comparison of the time series of offshore transport with depth of the 14°C isotherm indicates the opposite. Periods of strongest offshore transport correspond to periods of deepest depth of the 14°C isotherm. The 1957-1958, 1965, 1972-1973 and 1982-1983
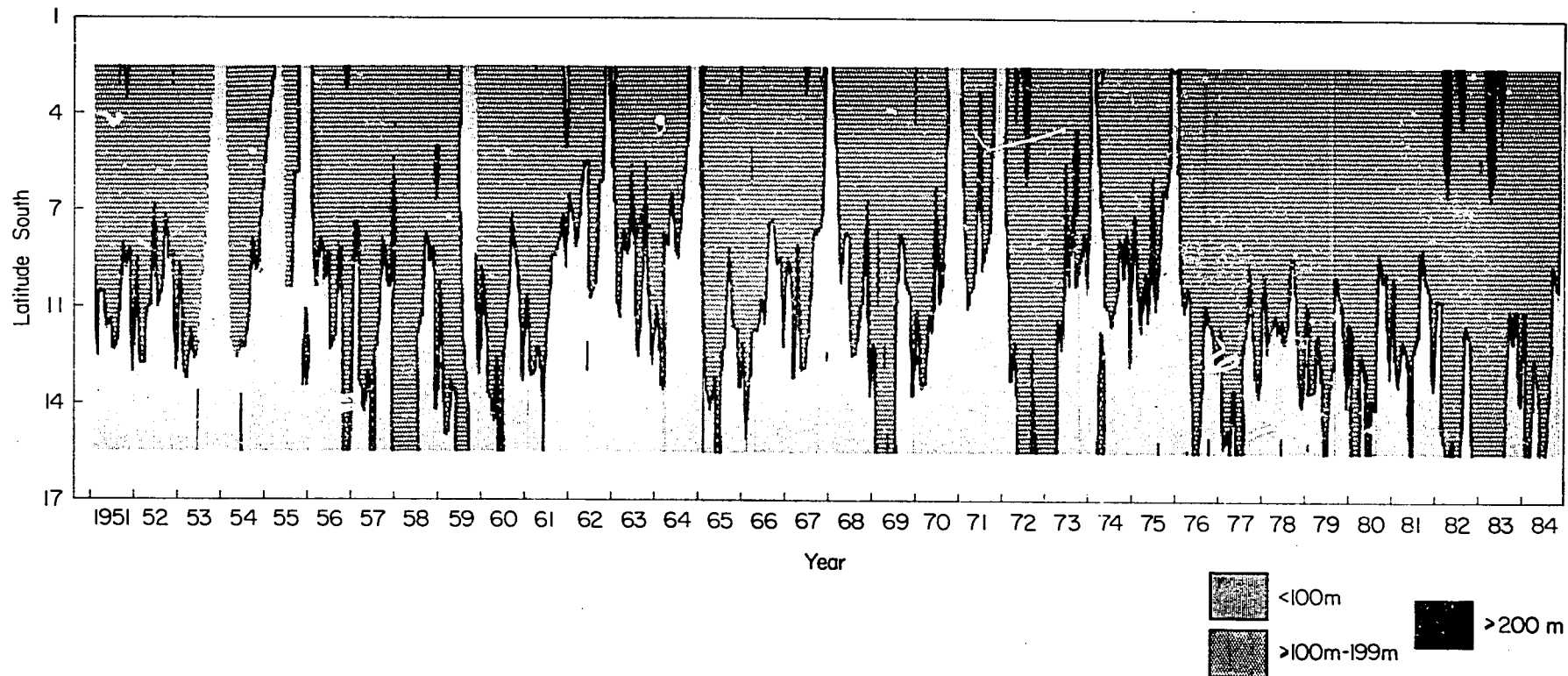
Fig. 11. Time-latitude contour plot of monthly mean depth of the 14°C isotherm for 5 areas along the coast off Peru. Data shown for "1951" are a composite of data for all years prior to 1952. The 14°C isotherm is generally shallower than 100 m in the south and deeper than 100 m in the north. The isotherm was occasionally deeper than 200 m in the northernmost areas (e.g., 1967, 1972, 1982 and 1983). Note the large region in the north during 1976-1984 when the 14°C isotherm was consistently deeper than 100 m.

Table 7. Monthly mean depth of the 14°C isotherm (m) for the region 4-14°S off Peru. These means are averages of the monthly means for the three central areas, computed from subsurface temperature profiles. The corresponding number of profiles used in computing each mean is printed (in brackets) to the right of the mean. Means based on zero profiles are computed from interpolated values. Asterisks indicate months in which neither observed nor interpolated means were available in all three areas.

Year	Jan	Feb	Mar	Apr	May	Jun	Jul	Aug	Sep	Oct	Nov	Dec
1951	96 (1)	112 (1)	108 (2)	116 (0)	121 (0)	110 (0)	149 (17)	126 (7)	96 (0)	96 (0)	**** (0)	**** (0)
1952	**** (0)	**** (0)	**** (0)	**** (0)	116 (0)	94 (0)	113 (144)	106 (0)	87 (0)	**** (0)	**** (0)	**** (0)
1953	101 (0)	115 (0)	127 (1)	123 (0)	123 (0)	**** (0)	**** (0)	**** (0)	**** (0)	**** (0)	**** (0)	**** (0)
1954	**** (0)	**** (0)	**** (0)	**** (0)	**** (0)	**** (0)	**** (0)	**** (0)	**** (0)	**** (0)	**** (0)	**** (0)
1955	**** (0)	**** (0)	**** (0)	**** (0)	**** (0)	**** (0)	**** (0)	**** (0)	81 (0)	73 (0)	73 (69)	85 (104)
1956	75 (5)	97 (0)	108 (0)	102 (47)	110 (0)	100 (0)	131 (0)	121 (0)	99 (30)	108 (0)	126 (5)	119 (0)
1957	98 (0)	90 (3)	118 (43)	135 (10)	127 (0)	108 (0)	**** (0)	**** (0)	94 (0)	98 (0)	102 (5)	105 (2)
1958	129 (41)	128 (9)	121 (65)	127 (6)	136 (2)	113 (0)	129 (1)	118 (0)	94 (51)	96 (0)	89 (5)	112 (173)
1959	101 (0)	120 (0)	148 (5)	129 (0)	125 (0)	**** (0)	**** (0)	**** (0)	**** (0)	**** (0)	**** (0)	113 (0)
1960	103 (0)	118 (3)	140 (32)	137 (75)	128 (3)	111 (0)	130 (0)	116 (0)	81 (7)	102 (94)	105 (33)	117 (0)
1961	109 (0)	126 (55)	134 (60)	131 (15)	127 (0)	105 (12)	121 (14)	104 (124)	96 (24)	82 (8)	91 (0)	98 (0)
1962	85 (63)	96 (77)	97 (24)	88 (90)	86 (101)	96 (20)	118 (35)	110 (0)	75 (0)	68 (20)	67 (284)	95 (54)
1963	66 (88)	113 (99)	115 (40)	93 (30)	104 (0)	90 (0)	96 (60)	143 (49)	101 (3)	86 (61)	110 (14)	132 (18)
1964	109 (0)	112 (11)	113 (13)	101 (0)	81 (51)	89 (99)	113 (2)	86 (59)	73 (61)	54 (9)	60 (180)	79 (0)
1965	80 (0)	114 (0)	125 (0)	119 (34)	132 (1)	109 (0)	136 (26)	130 (53)	103 (34)	123 (21)	124 (85)	145 (18)
1966	121 (0)	145 (47)	103 (42)	122 (32)	130 (44)	106 (21)	125 (0)	89 (5)	94 (135)	87 (2)	100 (29)	123 (41)
1967	99 (0)	109 (130)	120 (11)	107 (5)	142 (52)	114 (9)	126 (2)	95 (113)	90 (63)	88 (1)	79 (31)	81 (55)
1968	70 (0)	75 (114)	96 (1)	119 (7)	102 (32)	96 (0)	134 (0)	134 (0)	128 (57)	107 (32)	88 (9)	148 (37)
1969	130 (12)	109 (15)	148 (7)	130 (2)	134 (2)	123 (14)	125 (48)	97 (31)	101 (117)	102 (0)	113 (23)	148 (8)
1970	117 (0)	121 (0)	122 (0)	119 (0)	120 (1)	87 (26)	118 (0)	101 (0)	74 (67)	62 (95)	76 (125)	63 (47)
1971	71 (0)	100 (0)	114 (0)	109 (4)	101 (22)	79 (15)	111 (0)	98 (170)	90 (47)	60 (11)	69 (112)	74 (60)
1972	31 (1)	102 (20)	113 (49)	138 (59)	130 (17)	128 (0)	157 (25)	147 (15)	124 (0)	139 (22)	130 (87)	150 (2)
1973	121 (0)	141 (11)	134 (77)	124 (14)	121 (3)	90 (0)	100 (9)	86 (36)	95 (24)	94 (0)	93 (57)	101 (0)
1974	80 (2)	64 (24)	75 (40)	107 (7)	115 (7)	115 (15)	129 (5)	112 (5)	94 (0)	105 (3)	99 (0)	109 (0)
1975	95 (8)	105 (2)	121 (53)	102 (35)	116 (63)	92 (1)	118 (0)	99 (134)	81 (0)	80 (0)	59 (17)	76 (16)
1976	81 (0)	104 (0)	104 (6)	111 (11)	121 (0)	113 (0)	151 (21)	132 (14)	115 (0)	133 (23)	120 (0)	123 (12)
1977	113 (0)	139 (24)	133 (0)	128 (0)	127 (0)	123 (2)	135 (0)	120 (14)	101 (0)	114 (11)	122 (8)	121 (0)
1978	102 (0)	113 (1)	116 (5)	119 (0)	119 (2)	105 (0)	128 (1)	117 (0)	99 (0)	111 (0)	110 (0)	124 (0)
1979	106 (0)	*** (0)	*** (0)	*** (0)	*** (0)	110 (0)	139 (0)	138 (25)	105 (0)	108 (0)	128 (20)	124 (0)
1980	113 (0)	129 (4)	125 (14)	125 (0)	124 (0)	108 (0)	135 (0)	128 (11)	99 (0)	101 (0)	110 (0)	139 (3)
1981	102 (0)	119 (0)	133 (19)	126 (0)	124 (0)	*** (0)	*** (0)	*** (0)	97 (0)	105 (0)	*** (0)	*** (0)
1982	110 (0)	118 (5)	149 (29)	171 (19)	146 (0)	121 (0)	149 (0)	164 (14)	119 (0)	125 (0)	109 (33)	129 (17)
1983	154 (10)	180 (16)	168 (6)	185 (85)	169 (7)	151 (73)	166 (68)	134 (9)	114 (0)	125 (0)	156 (12)	151 (1)
1984	111 (0)	138 (18)	132 (0)	126 (0)	125 (0)	114 (0)	145 (14)	136 (10)	103 (0)	104 (0)	109 (7)	**** (0)

El Niño periods of anomalously deep thermocline occurred during the four highest peaks of offshore Ekman transport. Thus, the thermocline deepens sharply during periods when local wind forcing should produce anomalously shallow thermocline.

Depth of the SST-2ºC Isotherm

The depth of the SST-2ºC isotherm is an indicator of the thickness of the surface mixed layer, i.e., the depth to the top of the thermocline. The time series of monthly mean depth of the SST-2ºC isotherm (Fig. 4C, Table 8) show that variations in the depth of this isotherm occur over both seasonal and interannual time scales. Although anomalies (Fig. 5C) occurred during the major El Niño events, the interannual variations of the depth of the SST-2ºC isotherm are less closely correlated with El Niño events than were the other parameters discussed. Rather, the dominant interannual variations appear to occur over longer time scales. The SST-2ºC isotherm was anomalously shallow throughout most of the 1960s, anomalously deep from 1970 to 1976, near the long-term mean annual cycle from 1976 until 1982 and deep during the 1982-1983 El Niño.

The annual cycle of the depth of the SST-2ºC isotherm (Fig. 7C) is strong, varying from a minimum depth of 20-25 m from January through March (austral summer) to a maximum depth of 60-70 m from July through September (austral winter). This annual cycle corresponds well with Bakun's (this vol.) seasonal wind mixing index and surface wind stress calculations, further establishing the depth of the SST-2ºC isotherm as a reasonable measure of the mixed layer depth. Thus, the annual cycle of the depth of the SST-2ºC isotherm fluctuates with the upwelling cycle, being deep during the upwelling season and shallow during the nonupwelling season. Upwelling elevates the thermal structure in response to offshore transport of the surface water. The elevated thermal structure combined with increased turbulent mixing during the upwelling season apparently force the observed deepening of the SST-2ºC isotherm.

The between-year standard deviation and range between extrema vary between lows of about 5 and 20 m, respectively, in May and June to highs of about 20 and 40 m, respectively, in August and September (Fig. 7C). There is an inverse correlation between SST and depth of the SST-2ºC isotherm. The autocorrelation function of the depth of the SST-2ºC isotherm indicates weak persistence (Fig. 5C). This suggests that the mixed layer changes due to local rather than large-scale processes, which makes sense because it is primarily an indicator of the thickness of the wind forced mixed layer (or local upper layer stratification due to heat budget considerations).

Along the coast, the depth of the SST-2ºC isotherm slopes from a shallow annual mean depth in the north (Area I) of 31 m to a relatively deep annual mean depth in the south (Area V) of 50 m. The maximum coastwise between-year standard deviation occurs in August in Area II, which is located between the weak upwelling area to the north and the strong upwelling areas to the south, reflecting interannual variations in the northerly extent of the upwelling.

Heat Content from the Surface to the SST-2ºC Isotherm

The heat content from the surface down to the SST-2ºC isotherm (Fig. 4D) is computed as the vertically averaged mean temperature down to the SST-2ºC isotherm multiplied by that depth. Since the magnitudes of depth variations (in meters) are significantly greater than for temperature variations (in degrees Celsius), the computed heat contents are dominated more by depth than temperature. Thus, heat content is low (300 to 500ºC x m) during nonupwelling periods when the surface layer is warm but the SST-2ºC isotherm is very shallow. Conversely, heat content is high(>1,000ºC x m) during the upwelling regime when the surface layer is cool but the SST-2ºC isotherm is deep. Time series of monthly mean heat content (Fig. 4D, Table 9) and anomaly of heat content (Fig. 5D) reveal interannual variations almost identical to those described for the depth to the SST-2ºC isotherm.

The annual cycle of heat content has characteristics similar to the annual cycle described for depth to the SST-2ºC isotherm (Fig. 7D). The long-term mean values vary from about 500 mC

Table 8. Monthly mean depth of the SST-2°C isotherm (m) for the region 4-14°S off Peru. These means are averages of the monthly means for the three central areas, computed from subsurface temperature profiles. The corresponding number of profiles used in computing each mean (in brackets) is printed to the right of the mean. Means based on zero profiles are computed from interpolated values. Asterisks indicate months in which neither observed nor interpolated means were available in all three areas.

Year	Jan	Feb	Mar	Apr	May	Jun	Jul	Aug	Sep	Oct	Nov	Dec
1951	24 (1)	22 (1)	20 (195)	29 (0)	37 (0)	42 (0)	45 (34)	59 (6)	66 (0)	49 (0)	35 (0)	29 (0)
1952	13 (37)	17 (0)	20 (0)	** (0)	43 (0)	53 (0)	71 (143)	71 (0)	72 (0)	** (0)	** (0)	** (0)
1953	24 (0)	20 (0)	18 (62)	26 (145)	32 (24)	40 (0)	56 (0)	** (0)	** (0)	** (0)	** (0)	** (0)
1954	** (0)	** (0)	** (0)	** (0)	** (0)	** (0)	** (0)	** (0)	** (0)	** (0)	** (0)	** (0)
1955	** (0)	** (0)	** (0)	** (0)	** (0)	** (0)	** (0)	** (0)	66 (0)	45 (0)	32 (70)	31 (114)
1956	19 (5)	23 (0)	26 (0)	39 (47)	44 (0)	48 (0)	56 (0)	60 (0)	61 (31)	50 (0)	48 (15)	39 (0)
1957	26 (0)	20 (3)	28 (50)	25 (33)	38 (0)	45 (0)	** (0)	** (0)	69 (0)	53 (0)	42 (16)	48 (10)
1958	34 (78)	22 (16)	18 (90)	26 (8)	31 (4)	44 (0)	58 (4)	65 (0)	70 (54)	50 (0)	34 (5)	33 (174)
1959	24 (0)	23 (0)	23 (36)	34 (3)	43 (1)	47 (0)	58 (0)	64 (0)	71 (0)	60 (4)	40 (0)	36 (0)
1960	23 (0)	21 (7)	18 (47)	25 (107)	36 (4)	43 (0)	56 (0)	63 (0)	64 (10)	59 (92)	45 (49)	36 (0)
1961	19 (0)	14 (113)	16 (97)	25 (55)	35 (0)	40 (14)	63 (10)	62 (137)	70 (27)	39 (6)	32 (1)	32 (0)
1962	21 (102)	16 (130)	15 (35)	29 (100)	31 (107)	46 (36)	60 (27)	63 (0)	62 (0)	33 (20)	31 (273)	27 (58)
1963	16 (94)	19 (184)	19 (55)	22 (73)	34 (0)	42 (0)	54 (61)	62 (118)	54 (29)	67 (76)	36 (44)	36 (61)
1964	23 (0)	28 (13)	22 (47)	32 (0)	41 (54)	52 (95)	61 (3)	85 (37)	74 (40)	55 (7)	26 (182)	28 (2)
1965	20 (0)	25 (10)	21 (1)	32 (87)	40 (1)	41 (0)	47 (35)	48 (69)	52 (43)	50 (24)	37 (139)	35 (29)
1966	25 (0)	25 (96)	22 (65)	30 (34)	42 (69)	50 (25)	57 (0)	53 (4)	65 (130)	47 (0)	31 (29)	31 (50)
1967	20 (0)	18 (147)	24 (16)	25 (11)	41 (65)	50 (9)	69 (2)	76 (103)	86 (54)	52 (1)	42 (32)	37 (62)
1968	20 (0)	16 (120)	18 (1)	22 (7)	45 (41)	49 (0)	57 (0)	60 (0)	61 (73)	52 (36)	35 (11)	37 (73)
1969	** (17)	20 (23)	29 (8)	31 (2)	41 (3)	48 (20)	53 (58)	42 (34)	51 (149)	37 (0)	25 (59)	32 (19)
1970	22 (0)	23 (0)	22 (0)	32 (0)	40 (3)	50 (25)	60 (0)	65 (0)	74 (55)	41 (91)	47 (129)	31 (50)
1971	24 (0)	23 (0)	25 (0)	37 (12)	36 (28)	39 (23)	62 (0)	70 (172)	92 (46)	54 (8)	30 (118)	32 (58)
1972	21 (1)	22 (26)	25 (96)	36 (90)	40 (35)	45 (2)	54 (53)	53 (17)	70 (0)	48 (31)	53 (148)	53 (21)
1973	34 (6)	26 (15)	26 (114)	34 (25)	35 (3)	53 (0)	70 (11)	86 (38)	80 (25)	57 (0)	39 (0)	34 (0)
1974	21 (2)	18 (37)	21 (45)	40 (12)	44 (7)	45 (31)	64 (5)	65 (5)	73 (0)	62 (3)	43 (68)	38 (0)
1975	26 (8)	26 (2)	29 (56)	32 (45)	44 (64)	49 (1)	70 (0)	83 (141)	82 (0)	56 (0)	34 (15)	29 (19)
1976	22 (0)	23 (0)	28 (6)	30 (17)	38 (0)	44 (0)	57 (42)	59 (27)	67 (0)	42 (26)	38 (0)	** (17)
1977	26 (0)	29 (27)	25 (0)	31 (0)	37 (0)	41 (11)	59 (0)	66 (14)	68 (0)	41 (13)	36 (9)	34 (0)
1978	25 (0)	29 (1)	26 (5)	32 (0)	38 (2)	43 (0)	54 (4)	61 (0)	66 (0)	46 (0)	31 (21)	33 (0)
1979	23 (0)	** (0)	** (0)	** (0)	** (0)	43 (0)	52 (0)	52 (29)	63 (0)	47 (0)	35 (0)	28 (8)
1980	22 (0)	25 (4)	18 (17)	29 (0)	39 (0)	48 (0)	62 (0)	73 (13)	72 (0)	51 (0)	** (0)	** (0)
1981	22 (0)	19 (0)	13 (21)	27 (0)	38 (0)	** (0)	** (0)	** (0)	67 (0)	46 (0)	30 (36)	37 (19)
1982	24 (0)	24 (5)	24 (36)	27 (24)	39 (0)	45 (0)	58 (0)	63 (23)	74 (0)	64 (0)	59 (81)	57 (21)
1983	37 (14)	39 (32)	36 (6)	39 (99)	46 (7)	44 (99)	60 (80)	55 (11)	64 (0)	43 (13)	34 (0)	33 (0)
1984	23 (0)	20 (18)	21 (0)	30 (0)	38 (0)	41 (0)	46 (15)	59 (14)	66 (0)	49 (0)	37 (7)	** (0)

Table 9. Monthly mean heat content from the surface down to the SST-20°C isotherm (°C x m) for the region 4-14°S off Peru. These means are averages of the monthly means for the three central areas, computed from subsurface temperature profiles. The corresponding number of profiles used in computing each mean (in brackets) is printed to the right of the mean. Means based on zero profile are computed from interpolated values. Asterisks indicate months in which neither observed nor interpolated means were available in all three areas.

Year	Jan		Feb		Mar		Apr		May		Jun		Jul		Aug		Sep		Oct		Nov		Dec	
1951	491	(1)	524	(1)	506	(188)	609	(0)	748	(0)	772	(0)	801	(31)	1,063	(3)	984	(0)	837	(0)	596	(0)	553	(0)
1952	270	(37)	401	(0)	440	(0)	***	(0)	789	(0)	895	(0)	1,154	(122)	1,069	(0)	1,036	(0)	***	(0)	***	(0)	***	(0)
1953	458	(0)	465	(0)	419	(59)	558	(137)	613	(24)	748	(0)	984	(0)	***	(0)	***	(0)	***	(0)	***	(0)	***	(0)
1954	***	(0)	***	(0)	***	(0)	***	(0)	***	(0)	***	(0)	***	(0)	***	(0)	***	(0)	***	(0)	***	(0)	***	(0)
1955	***	(0)	***	(0)	***	(0)	***	(0)	***	(0)	***	(0)	***	(0)	***	(0)	974	(0)	763	(0)	568	(59)	594	(113)
1956	371	(5)	495	(0)	552	(0)	728	(44)	832	(0)	865	(0)	1,011	(0)	1,000	(0)	1,039	(30)	886	(0)	809	(14)	730	(0)
1957	514	(0)	436	(3)	683	(45)	560	(33)	771	(0)	822	(0)	***	(0)	***	(0)	1,012	(0)	864	(0)	664	(14)	831	(5)
1958	737	(64)	515	(15)	441	(83)	527	(8)	670	(2)	813	(0)	967	(2)	1,003	(0)	1,001	(40)	834	(0)	610	(4)	689	(171)
1959	510	(0)	549	(0)	548	(35)	697	(3)	876	(1)	856	(0)	1,020	(0)	1,012	(0)	1,031	(0)	937	(3)	673	(0)	664	(0)
1960	436	(0)	472	(6)	336	(42)	496	(101)	659	(4)	780	(0)	984	(0)	975	(0)	947	(9)	850	(83)	698	(42)	632	(0)
1961	341	(0)	280	(109)	318	(94)	429	(52)	632	(0)	664	(14)	998	(8)	994	(126)	1,101	(25)	652	(6)	577	(1)	593	(0)
1962	425	(102)	326	(129)	309	(35)	507	(100)	570	(98)	797	(32)	985	(24)	963	(0)	895	(0)	558	(17)	555	(246)	541	(58)
1963	314	(87)	435	(183)	413	(55)	391	(72)	650	(0)	774	(0)	946	(59)	980	(107)	857	(28)	952	(71)	625	(42)	663	(59)
1964	440	(0)	578	(12)	419	(46)	542	(0)	652	(42)	861	(81)	1,034	(3)	1,015	(26)	990	(33)	734	(3)	452	(179)	541	(2)
1965	409	(0)	600	(9)	509	(1)	752	(76)	822	(0)	816	(0)	924	(30)	890	(57)	827	(43)	864	(24)	641	(121)	697	(27)
1966	475	(0)	535	(96)	434	(60)	599	(33)	673	(59)	828	(24)	953	(0)	857	(3)	988	(114)	794	(0)	560	(27)	602	(50)
1967	400	(0)	404	(142)	558	(15)	496	(9)	774	(65)	881	(8)	1,132	(2)	1,079	(79)	1,197	(43)	845	(1)	673	(31)	670	(62)
1968	380	(0)	340	(199)	385	(1)	463	(4)	753	(40)	827	(0)	1,023	(0)	1,040	(0)	1,097	(67)	897	(33)	611	(11)	678	(65)
1969	458	(46)	431	(21)	588	(6)	602	(2)	824	(3)	898	(19)	950	(53)	748	(26)	851	(145)	669	(0)	447	(58)	555	(14)
1970	415	(0)	498	(0)	490	(0)	604	(0)	797	(2)	834	(23)	992	(0)	974	(0)	1,024	(38)	665	(72)	693	(112)	557	(49)
1971	421	(0)	474	(0)	459	(0)	568	(10)	672	(25)	711	(20)	1,014	(0)	1,039	(141)	1,053	(39)	844	(8)	522	(116)	582	(52)•
1972	427	(1)	504	(25)	573	(85)	780	(76)	799	(30)	880	(2)	1,130	(45)	921	(17)	1,054	(0)	842	(27)	922	(108)	930	(8)
1973	605	(4)	599	(13)	539	(109)	613	(25)	762	(1)	893	(0)	1,167	(10)	1,117	(23)	1,045	(19)	864	(0)	656	(0)	618	(0)
1974	435	(2)	317	(36)	452	(44)	582	(10)	875	(7)	856	(23)	1,100	(5)	1,024	(5)	1,070	(0)	1,049	(3)	711	(64)	698	(0)
1975	504	(6)	592	(2)	684	(55)	677	(42)	806	(55)	868	(1)	1,095	(0)	1,131	(115)	1,102	(0)	864	(0)	557	(15)	548	(18)
1976	431	(0)	514	(0)	612	(6)	596	(17)	771	(0)	872	(0)	1,127	(38)	1,083	(25)	1,045	(0)	786	(23)	688	(0)	760	(30)
1977	570	(0)	707	(26)	579	(0)	626	(0)	734	(0)	771	(11)	1,019	(0)	1,021	(0)	1,037	(9)	906	(11)	653	(9)	674	(0)
1978	501	(0)	658	(1)	542	(5)	627	(0)	797	(2)	799	(0)	949	(4)	960	(0)	979	(0)	809	(0)	592	(21)	648	(0)
1979	470	(0)	***	(0)	***	(0)	***	(0)	***	(0)	818	(0)	999	(0)	988	(26)	1,009	(0)	828	(0)	623	(0)	564	(8)
1980	462	(0)	605	(4)	447	(17)	593	(0)	759	(0)	849	(0)	1,051	(0)	1,040	(11)	1,027	(0)	838	(0)	***	(0)	***	(0)
1981	438	(0)	430	(0)	303	(21)	519	(0)	727	(0)	***	(0)	***	(0)	***	(0)	993	(0)	815	(0)	594	(35)	776	(19)
1982	494	(0)	525	(5)	488	(35)	596	(24)	768	(0)	854	(0)	1,070	(0)	1,135	(23)	1,117	(0)	1,022	(0)	1,056	(32)	832	(7)
1983	663	(6)	849	(14)	688	(1)	883	(63)	957	(3)	988	(59)	1,067	(50)	1,017	(8)	982	(0)	782	(13)	617	(0)	641	(7)
1984	456	(0)	464	(16)	476	(0)	590	(0)	735	(0)	777	(0)	855	(11)	1,006	(12)	997	(0)	848	(0)	680	(7)	***	(0)

from January through March to about 1,000 °Cm from July through September. The between-year standard deviation varies from about 100 °Cm in June to about 200 °Cm in November and February. The range between extrema varies from 200 to 600 °Cm. The autocorrelation function of heat content is 0.5 at lag one and decreases rapidly thereafter, indicating weak persistence with time (Fig. 5D). Along the coast, the long-term monthly means of heat content generally slope downward to the south. For instance, the long-term annual mean heat contents for Area I in the north and Area V in the south are 582 °Cm and 843 °Cm, respectively. This alongshore variation is a consequence of the deepening of the mixed layer in response to upwelling, which is stronger in the south. The interannual variability of the heat content is highest in areas and months around the edges of the upwelling regime.

Sea Level

Sea level represents a vertical integr?' of the thermohaline structure over the entire water column. Integrating over the water column has the effect of combining many subsurface processes into a single parameter. Frequently, this combining of factors provides an invaluable indication of large-scale oceanic change. Monthly means and anomalies of sea level at Talara and La Punta (Figs. 1D, 1E and 2D, 2E, Tables 4 and 5) show seasonal and interannual variability similar to that described for SST. Sea level at both coastal stations was variable during the early 1950s, moderately low during the mid-1950s, moderately high for the 1957-1959 El Niño episode, slightly below normal for most of the 1960s (except the 1965 and 1969 warm events when it was above normal), very high during the 1972-1973 El Niño, and variable until 1974.

The annual cycle of sea level is characterized by relatively high levels from February through June and low levels from August through December. The interannual variability is generally high from December through June and low from August through September. Bigg and Gill (1986) showed that the long period response of sea level off Peru separates into a remotely forced component mainly due to zonal winds along the equator to the west, and a locally driven component where sea level slopes to balance the alongshore wind. Their examination of the annual component of sea level indicates that the locally forced component dominates, whereas the remotely forced component plays a major role at semiannual and interannual periods.

Summary and Implications

All of the time series presented show considerable seasonal and interannual variability. Each series had a strong annual cycle, dominated by seasonal shifts from an intensified upwelling regime from May to October to a relaxed upwelling regime in which warm water intrudes from the north from January through March. Contrary to this single peak pattern observed for SOI, SST, sea level, depth to the SST-2°C isotherm, and heat content, deep isotherms, represented by the depth of the 14°C isotherm, had double peaks in their annual cycles. Along the Peru coast, the seasonal variability increased from north to south, with lowest variability associated with weaker upwelling in the north than in the south.

Interannual variations of most of the series were similar, being dominated by remotely-forced El Niño signals. Contrary to this pattern, however, interannual variations of the depth to the SST-2°C isotherm and heat content down to this isotherm were only weakly correlated to El Niño signals. Interannual variations of these two parameters appear to occur at longer periods. Weaker persistence suggests that these two parameters may be dominated by local rather than large-scale processes, such as local wind or heating events. The parameters which were correlated to El Niño signals showed that coastal waters off Peru (4-14°S) were generally cool in the early 1950s, moderately warm during 1957-1959, near normal during 1960-1965, warm in 1965, near normal during 1966-1968, warm in 1969, cool in 1970 and 1971, very warm in 1972, cool during 1973-1975, warm during 1976-1981, extremely warm in 1982-1983 and variable in 1984. La Punta SST was below normal in 1984-1985, but the 14°C isotherm was still depressed.

The warm events described by the above interannual variations represent a general deepening of the thermal structure along the coast as indicated by a depression of the 14oC isotherm. Such depressions cause a change in the slope of the thermal structure normal to the coast and a tendency to increase transport of warm water and associated organisms poleward along the coast. Furthermore, deepening the thermal structure would reduce the biological productivity of the surface waters by reducing the ability or upwelling favorable winds to upwell nutrient-rich water. These depressions of the thermal structure have been shown to occur even during periods of maximum offshore transport, which normally correspond to maximum upwelling and availability of nutrients.

The effects of interannual variability of subsurface temperature on Peruvian anchoveta populations are difficult to access. If one assumed that some combination of factors associated with warming and depression of the thermal structure is detrimental to anchoveta recruitment and/or growth, a scenario of events based on the subsurface variability presented here may be as follows. Heavy fishing pressure in the late 1960s and early 1970s combined with the strong El Niño of 1972, which had a deeply depressed thermal structure, caused a collapse of the anchoveta population. The stock then recovered slightly in 1974-1976 (Avaria 1985) following cool water conditions (upwelling) of 1973-1975 as described by the depression of the 14oC isotherm. However, this slight recovery was subject to continued strong fishing pressure. The moderate 1976-1977 El Niño and the warm, depressed conditions thereafter, especially during the 1982-1983 El Niño, have prevented good recruitment, resulting in very low anchoveta populations. A reversal to cooler conditions since 1983 may be associated with a modest recent recovery of the population. Clearly, the actual ecosystem of the Peruvian anchoveta is much more complicated than this simple scenario suggests. This scenario does, however, illustrate the potential value of multiple environmental time series such as presented in this volume.

Acknowledgements

References

Avaria, S. 1985. Effects of "El Niño" on Southeast Pacific fisheries. Estudio Regional Del Fenomeno El Niño, Boletin 13:17-26.

Barber, R.T., F.P. Chavez and J.E. Kogelschatz, 1985. Biological effects of El Niño. Estudio Regional del Fenomeno El Niño, Boletin 14:3-29.

Barilotti, D.C., D.R. McLain and R.A. Bauer. 1984. Forecasting standing crops of *Macrocystis pyrifera* from the depth of the 14oC isotherm. (Abstract L 032A-06) EOS-Trans. Amer. Geophys. Union 65(45):909.

Bigg, G.R. and A.E. Gill. 1986. The annual cycle of sea level in the eastern Tropical Pacific. J. Phys. Oceanogr. 16(2):1055-1061.

Brainard, R.E. and D.R. McLain. 1985. Surbsurface temperature variability along the west coast of North and south America. Trop. Ocean-Atmosphere Newsl. 31:1-2.

Cane, M.A. 1983. Oceanographic events during El Niño. Science (Wash.) 222:1189-1195.

Chavez, F.P., R.T. Barber and H.S. Soldi. 1984. Propagated temperature changes during onset and recovery of the 1982-1983 El Niño. Nature 309:47-49.

Enfield, D.B. and J.S. Allen. 1980. On the structure and dynamics of monthly mean sea level anomalies along the Pacific coast of North and South America. J. Phys. Oceanogr. 10(4):557-578.

Gunther, E.R. 1936. A report on oceanographical evaluation in the Peru coastal current. Discovery Report 13:107-276.

McCreary, J.P. 1976. Eastern tropical ocean response to changing wind systems: with application to El Niño. J. Phys. Oceanog. 6:632-645.

McLain, D.R. 1983. Coastal ocean warming in the northeast Pacific, 1976-83, p. 61-86. In W.G. Pearcy (ed.) The influence of oceanic conditions on the production of salmonids in the North Pacific, a workshop. Sea Grant College Program. Rep. ORESU-W-83-001. Oregon State Univ., Newport.

Meyers, G. 1979. Annual variation in the slope of the 14oC isotherm along the equator in the Pacific Ocean. J. Phys. Oceanogr. 9(5):885-891.

Norton, J., D.R. McLain, R.E. Brainard and D. Husby, 1984. The 1982-83 El Niño event off Baja and Alta California and its ocean climate context, p. 44-72. In W.S. Wooster and D.L. Fluharty (eds.) El Niño north: Niño effects in the subarctic Pacific Ocean. Washington Sea Grant Program, University of Washington.

Parrish, R.H., A. Bakun, D.M. Husby and C.S. Nelson. 1983. Comparative climatology of selected environmental processes in relation to eastern boundary pelagic fish reproduction. *In* G.D. Sharp and J. Csirke (eds.) Proceedings of the Expert Consultation to Examine Changes in Abundance and Species Composition of Neritic Fish Resources, San José, Costa Rica, April 1983. FAO Fish. Rep. 291(3):731-777.

Quinn, W.H. 1974. Monitoring and predicting El Niño invasions. J. Appl. Meteor. 13:825-830.

Quinn, W.H. and V.T. Neal. 1983. Long-term variations in the southern oscillation. El Niño and Chilean sub-tropical rainfall. Fish. Bull. 81:363-373.

Rasmusson, E.M. 1984. El Niño: the ocean/atmosphere connection. Oceanus 27(2):5-12.

Reinecker, M.M. and C.N.K. Mooers. 1986. The 1982-83 El Niño signal off northern California. J. Geophys. Res. 91(C5):6597-6608.

Robinson, M.K. and R.A. Bauer. 1976. Atlas of North Pacific Ocean monthly mean temperatures and mean salinities of the surface layer. Reference Publication 2. Naval Oceanographic Office. Washington, DC. 192 p.

Ryther, J.H., D.W. Menzel, E.M. Hulburt, C.J. Lorenzen and N. Corwin. 1971. The production utilization of organic matter in the Peru coastal current. Invest. Pesq. 35:43-59.

Teague, W.J., R.L. Pickett and O.A. Burns. 1985. Editing the master oceanographic observations data set (MOODS), p. 294-297. *In* Proceedings of the 1985 Symposium, Ocean Data: Sensor-to-User. Marine Technology Society, Gulf Coast Section.

Wyrtki, K. 1965. Surface currents in the eastern tropical Pacific Ocean. Bull. Inter-Amer. Trop. Tuna Comm. 9(5):271-304.

Wyrtki, K. 1966. Oceanography of the eastern equatorial Pacific Ocean. Oceanogr. Mar. Biol. Ann. Rev. 4:33-68.

Wyrtki, K. 1975. El Niño: the dynamical response of the equatorial Pacific Ocean to atmospheric forcing. J. Phys. Oceanogr. 5(4):572-584.

Wyrtki, K. and S. Nakahara. 1984. Monthly maps of sea level anomalies in the Pacific, 1975-81. HIG-84-03, 93 p., Hawaii Institute of Geophysics, Univ. of Hawaii.

The Peruvian Anchoveta
and Its Upwelling Ecosystem:
Three Decades of Change

Edited by

D. Pauly and I. Tsukayama

1987

The Peruvian Anchoveta
and Its Upwelling Ecosystem:
Three Decades of Change

EDITED BY

D. PAULY
I. TSUKAYAMA

1987

Cover: Time series of turbulence *(above)* and sea surface temperature *(below)*, combined with pre-hispanic representation of Peruvian
fisherman, adapted from IMARPE report entitled "Research on the Anchovy: Models and Reality" (1975).
Artwork by Ovidio F. Espiritu, Jr.